Journal of Medicinal Chemistry

ARTICLE

pubs.acs.org/jmc

New 2-Heterocyclyl-imidazo[2,1-*i*]purin-5-one Derivatives as Potent and Selective Human A_3 Adenosine Receptor Antagonists

Pier Giovanni Baraldi,[*,†] Delia Preti,[*,†] Abdel Naser Zaid,[§] Giulia Saponaro,[†] Mojgan Aghazadeh Tabrizi,[†] Stefania Baraldi,[†] Romeo Romagnoli,[†] Allan R. Moorman,[∥] Katia Varani,[‡] Sandro Cosconati,[#] Salvatore Di Maro,[⊥] Luciana Marinelli,[⊥] Ettore Novellino,[⊥] and Pier Andrea Borea[‡]

[†]Dipartimento di Scienze Farmaceutiche, [‡]Dipartimento di Medicina Clinica e Sperimentale-Sezione di Farmacologia, Università di Ferrara, Via Fossato di Mortara 17-19, 44121 Ferrara Italy

[§]College of Pharmacy, An-Najah National University, Nablus, Palestine

[∥]King Pharmaceutical R & D, 4000 CentreGreen Way, Suite 300 Cary, North Carolina 27513, United States

[⊥]Dipartimento di Chimica Farmaceutica e Tossicologica, Università "Federico II", Via D. Montesano 49, 80131 Napoli, Italy

[#]Dipartimento di Scienze Ambientali, Seconda Università di Napoli, Via Vivaldi 43, 81100 Caserta, Italy

Supporting Information

ABSTRACT: A series of 4-allyl/benzyl-7,8-dihydro-8-methyl/ethyl-2-[(substituted)isoxazol/pyrazol-3/5-yl]-1*H*-imidazo[2,1-*i*]-purin-5(4*H*)-ones has been synthesized and evaluated in radioligand binding assays to determine their affinities at the human A_1, A_{2A}, and A_3 adenosine receptors. Efficacy at the hA_{2B} AR and antagonism of selected ligands at the hA_3 AR were also assessed through cAMP experiments. All of the synthesized molecules exhibited high affinity at the hA_3 AR (K_i values ranging from 1.46 to 44.8 nM), as well as remarkable selectivity versus A_1, A_{2A}, and A_{2B} AR subtypes. Compound (*R*)-4-allyl-8-ethyl-7,8-dihydro-2-(3-methoxy-1-methyl-1*H*-pyrazol-5-yl)-1*H*-imidazo[2,1-*i*]purin-5(4*H*)-one (*R*-**33**) was found to be the most potent and selective ligand of the series (K_i hA_3 = 1.46 nM, K_i hA_{2A}/K_i hA_3 > 3425; IC_{50} hA_{2B}/K_i hA_3 > 3425; K_i hA_1/K_i hA_3 = 1729). Molecular modeling studies were helpful in rationalizing the available structure−activity relationships along with the selectivity profiles of the new series of ligands.

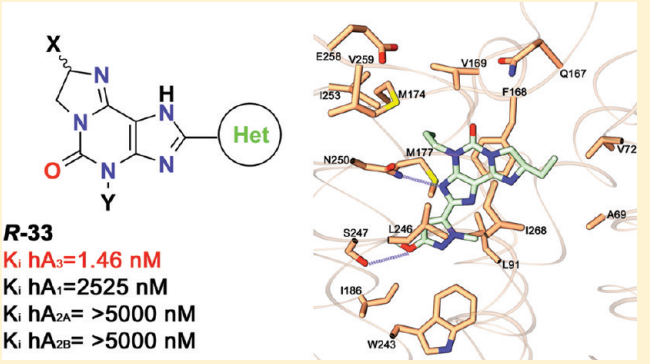

INTRODUCTION

Adenosine exerts a number of physiological functions through activation of four cell membrane G-protein-coupled receptors classified as A_1, A_{2A}, A_{2B}, and A_3 (ARs).[1] The A_3 AR has been the subject of intensive investigations over the past decade as a potential therapeutic target due to its contribution to important pathophysiological processes.[2]

The clarification of the role of adenosine and its receptors in cancer development may hold great promise for the chemotherapeutic treatment of patients affected by malignancies.[3] It has been suggested that adenosine inhibits tumor cell growth while maintaining bone marrow cell proliferation through the involvement of the A_3 receptors.[4] Evidence of high levels of expression of A_3 adenosine receptor subtype has been provided in several tumor cell lines, and A_3 specific antagonists seem to synergistically enhance cytotoxic treatment and counter P-glycoprotein efflux in multidrug resistance.[5−7] A recent study provides the first evidence that the A_3 AR plays a role in colon tumorigenesis and, more importantly, can potentially be used as a diagnostic marker or a therapeutic target for colon cancer.[8]

Although many different chemical classes have been identified as A_3 AR antagonists, few have reached the preclinical phase of investigation, possibly due to the enigmatic physiological role of A_3 AR, whose activation seems related to opposite effects concerning tissue protection in inflammatory and cancer cells. A_3 AR antagonists are currently under biological testing for their promising therapeutic potential in the treatment of inflammation, neurodegeneration, ischemia, asthma, glaucoma, and cancer.[8−11]

A wide number of compounds exerting high potency and selectivity in antagonizing the hA_3 AR has been identified.[12,13] Aromatic nitrogen-containing monocyclic (i.e., thiazoles, thiadiazoles,[14] 1,4-dihydropyridines,[15] pyridines,[16] 2-mercaptopyrimidines[17]), bicyclic (i.e., flavonoid,[18] isoquinoline, quinozalines,[19] (aza)adenines[20]), tricyclic systems (i.e., pyrazoloquinolines,[21,22] triazoloquinoxalines,[23] pyrazolotriazolopyrimidines,[24] triazolopurines,[25] tricyclic xanthines[26−28]), and nucleoside-derived antagonists[29−31] have been reported as A_3 AR ligands.

Received: April 20, 2011
Published: June 15, 2011

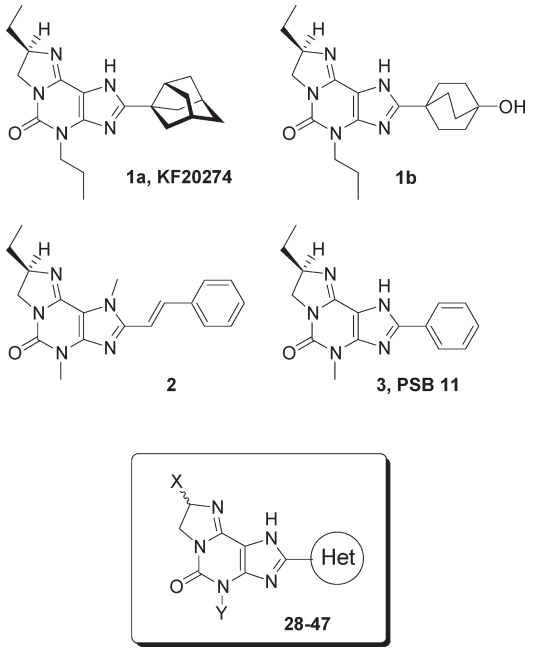

Figure 1. 2-Substituted-imidazo[2,1-*i*]purin-5-one derivatives as ARs antagonists.

Scheme 1. Synthesis of the Described 2-Heterocyclyl-imidazo[2,1-*i*]purin-5-one Derivatives[a]

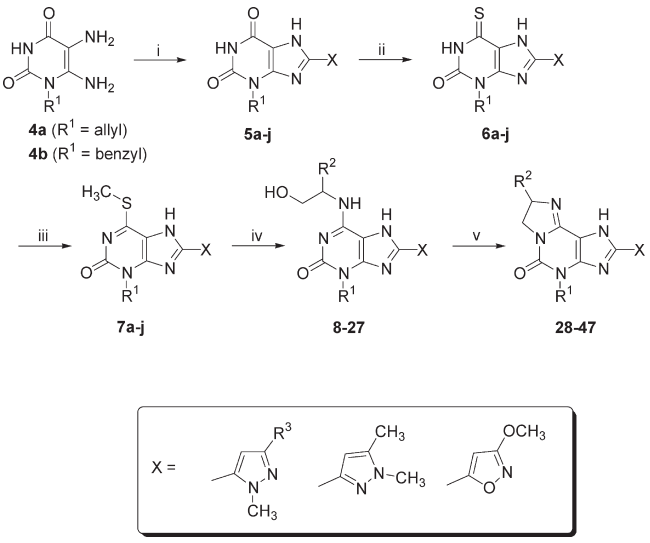

[a] Reagents: (i) (a) XCOOH, EDAC, HOBt, DMF, rt, 24 h; (b) NaOH 10%, reflux, 1.5 h; (ii) P_2S_5, pyridine, 140 °C, 5 h; (iii) CH_3I, NaOH/EtOH, rt, 3 h; (iv) (*R*/*S*/*R*,*S*)-2-amino-butan/propan-1-ol, DMSO, 150 °C, 1 h; (v) $SOCl_2$, CH_2Cl_2, reflux, 18 h.

We focused our attention on the imidazo[2,1-*i*]purin-5-one scaffold, obtained by the fusion of an imidazoline ring on the xanthine bicycle, as an interesting tricyclic structure useful for the development of ARs ligands. Particular attention has been paid to substitution at the 2-position of the imidazo[2,1-*i*]purinone nucleus, which theoretically corresponds to the 8-position of the original xanthine core. It has been established that the 2-substituent plays a crucial role in the subtype selectivity of the AR antagonists reported so far.[32−37] Compound **1a** (KF20274, Figure 1),[32] substituted at the 2-position with a 3-noradamantyl moiety, can be structurally associated to the previously reported A_1 antagonist 1,3-dipropyl-8-(3-noradamantyl)xanthine.[32] Thus, the 3-noradamantyl function was shown to induce A_1 selective antagonist activity in both the tricycle **1a** and the corresponding xanthine analogue. The main advantage claimed for the annelation of the xanthine core into the imidazo[2,1-*i*]purinone scaffold is the enhancement of water solubility afforded by the imidazoline basic nitrogen, which has been reported to be subject to protonation at physiological pH. Compound **1b**, (*R*)-7,8-dihydro-8-ethyl-2-(4-bicyclo[2.2.2]octan-1-ol)-4-propyl-1*H*-imidazo[2,1-*i*]purin-5(4*H*)-one,[33] is a particularly potent A_1 AR antagonist with good selectivity over the other three AR subtypes and high water solubility (>100 mg/mL) and showed a good in vivo profile after oral administration in a rat diuresis model. Müller and co-worker explored the imidazopurinone nucleus, introducing at the 2-position substituents previously known to promote A_{2A} or A_3 AR activity in the corresponding 8-substituted xanthine analogues.[35] Compound **2** (Figure 1) was conceived as a water-soluble tricyclic congener of 8-styrylxanthines with A_{2A} AR antagonist properties, while derivative **3** (PSB11,[35] (*R*)-4-methyl-8-ethyl-2-phenyl-4,5,7,8-tetrahydro-1*H*-imidazo[2,1-*i*]purin-5-one) exhibited a K_i value of 2.3 nM for A_3 receptor. The radiolabeled derivative of this compound exhibited a K_D value of 4.9 nM and a B_{max} value of 3500 fmol/mg of protein.[36] The 2-(2,3,5-trichlorophenyl) substituted analogue, PSB10,[37] showed inverse agonist activity in binding studies in CHO cells expressing recombinant hA_3 ARs (IC_{50} = 4 nM).

In a recent study, we synthesized a wide series of 8-heterocyclyl-substituted xanthine derivatives, among which we identified very potent and selective human A_{2B} AR antagonists.[38] With this series, whose design was based on the structure of the 8-phenyl-xanthine derivative MRS1754 (*N*-(4-cyanophenyl)-2-[4-(2,3,6,7-tetrahydro-2,6-dioxo-1,3-dipropyl-1*H*-purin-8-yl)-phenoxy]acetamide),[39] we demonstrated that the phenyl and the pyrazole rings may occasionally behave as bioisosters. Given these findings, in the present study, we evaluated the effect of the replacement of the 2-phenyl ring of **3** and congeners with differently substituted 5-membered heterocycles, in particular 1,3- and 1,5-disubstituted pyrazoles or a 3-substituted isoxazole (Figure 1). At the 4-position, an allyl or a benzyl group have been introduced, while the 8-position has been functionalized with a methyl or an ethyl group, as the efficacy of such substituents was suggested by previous SAR studies on a different series of xanthine-related ARs antagonists. To verify a possible enantioselective interaction between the newly reported series of imidazo[2,1-*i*]purinones and ARs, the pharmacological properties of the optically pure enantiomers have been compared to those of the corresponding racemates for a select number of compounds. Moreover, molecular modeling studies were helpful in rationalizing the available structure−activity relationships along with the selectivity profiles of the new series of ligands.

CHEMISTRY

The synthesis of the 2-heterocyclyl tricyclic purinone derivatives has been performed, in analogy to described procedures, as depicted in Scheme 1.[32,35,37,40] 1-Subsituted-5,6-diaminouracils **4a**,**b**[41] and the appropriate pyrazole/isoxazole carboxylic acids were reacted in DMF solution in the presence of 1-ethyl-3-[3(dimethylamino)propyl]carbodiimide hydrochloride (EDAC)

dx.doi.org/10.1021/jm2004738 |*J. Med. Chem.* 2011, 54, 5205–5220

Table 1. Binding (hA_1, hA_{2A}, and hA_3) and Functional (hA_{2B}, hA_3) Parameters of the Synthesized 2-Heterocyclyl-imidazo[2,1-*i*]purin-5-one Derivatives Towards Adenosine Receptors

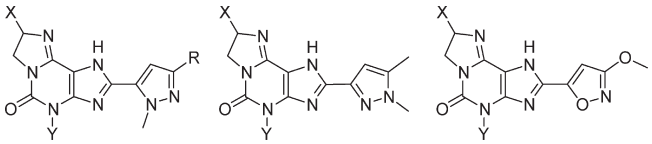

28-39 **40-43** **44-47**

compd	X	Y	R	hA_1 (K_i nM)[a]	hA_{2A} (K_i nM)[b]	A_{2B} (IC_{50} nM)[c]	hA_3 (K_i nM)[d]	hA_3 (IC_{50} nM)[e]
28	Me	allyl	Me	2040 (1710−2450)	>5000 (7%)	>5000 (30%)	4.56 (3.44−6.05)	34.2 (27.4−42.6)
R-**28**	Me	allyl	Me	2510 (2050−3060)	>5000 (1%)	>5000 (10%)	5.04 (5.14−6.01)	35.9 (29.9−43.0)
S-**28**	Me	allyl	Me	1960 (1540−2480)	>5000 (4%)	>5000 (12%)	6.03 (5.64−6.38)	40.9 (34.9−47.9)
29	Et	allyl	Me	515 (437−608)	>5000 (8%)	>5000 (20%)	3.01 (2.29−3.96)	30.3 (26.0−35.2)
30	Me	Bn	Me	>5000 (20%)	>5000 (1%)	>5000 (8%)	17.2 (12.2−24.0)	nd[f]
31	Et	Bn	Me	615 (536−707)	>5000 (5%)	>5000 (20%)	10.3 (7.9−13.4)	nd
R-**31**	Et	Bn	Me	803 (654−986)	>5000 (3%)	>5000 (10%)	12.6 (9.4−16.9)	nd
S-**31**	Et	Bn	Me	545 (468−635)	>5000 (4%)	>5000 (13%)	13.2 (9.7−17.9)	nd
32	Me	allyl	OMe	>5000 (30%)	>5000 (1%)	>5000 (13%)	2.36 (1.60−3.49)	14.5 (10.5−20.1)
33	Et	allyl	OMe	1530 (1280−1830)	>5000 (1%)	>5000 (16%)	1.96 (1.22−3.13)	12.2 (8.4−17.7)
R-**33**	Et	allyl	OMe	2525 (2106−3027)	>5000 (13%)	>5000 (21%)	1.46 (0.88−2.42)	23.4 (16.7−32.9)
S-**33**	Et	allyl	OMe	1078 (868−1340)	>5000 (15%)	>5000 (14%)	2.37 (1.48−3.83)	10.5 (7.4−14.9)
34	Me	Bn	OMe	1900 (1720−2090)	>5000 (1%)	>5000 (11%)	3.11 (2.01−4.80)	27.6 (23.3−32.7)
R-**34**	Me	Bn	OMe	2550 (2060−3170)	>5000 (11%)	>5000 (19%)	2.38 (1.79−3.17)	15.9 (12.6−20.1)
S-**34**	Me	Bn	OMe	1730 (1470−2030)	>5000 (1%)	>5000 (22%)	2.52 (1.64−3.88)	17.5 (13.4−22.9)
35	Et	Bn	OMe	405 (338−486)	>5000 (9%)	>5000 (22%)	3.85 (3.14−4.72)	20.4 (14.3−29.1)
36	Me	allyl	OBn	>5000 (47%)	>5000 (25%)	>5000 (17%)	24.7 (17.0−35.8)	nd
37	Et	allyl	OBn	1200 (1030−1400)	>5000 (5%)	>5000 (14%)	21.5 (17.0−27.3)	nd
38	Me	Bn	OBn	2560 (2300−2860)	2010 (1720−2360)	>5000 (13%)	44.8 (36.5−55.0)	nd
39	Et	Bn	OBn	1680 (1380−2040)	2130 (1870−2430)	>5000 (12%)	39.8 (31.6−50.1)	nd
40	Me	allyl		>5000 (13%)	>5000 (1%)	>5000 (9%)	13.9 (10.7−18.1)	nd
41	Et	allyl		>5000 (20%)	>5000 (1%)	>5000 (16%)	12.5 (8.6−18.2)	nd

dx.doi.org/10.1021/jm2004738 |*J. Med. Chem.* 2011, 54, 5205–5220

Table 1. Continued

compd	X	Y	R	hA_1 (K_i nM)[a]	hA_{2A} (K_i nM)[b]	A_{2B} (IC_{50} nM)[c]	hA_3 (K_i nM)[d]	hA_3 (IC_{50} nM)[e]
R-**41**	Et	allyl		>5000 (12%)	>5000 (3%)	>5000 (14%)	12.2 (8.4−17.7)	nd
S-**41**	Et	allyl		>5000 (29%)	>5000 (1%)	>5000 (8%)	9.20 (7.61−11.12)	nd
42	Me	Bn		>5000 (22%)	>5000 (9%)	>5000 (24%)	12.20 (8.4−17.7)	nd
43	Et	Bn		>5000 (28%)	>5000 (13%)	>5000 (27%)	15.0 (13.3−16.9)	nd
44	Me	allyl		>5000 (26%)	>5000 (11%)	>5000 (13%)	3.58 (2.84−4.51)	24.2 (19.1−30.7)
45	Et	allyl		3023 (2388−3827)	1520 (1126−2051)	>5000 (25%)	1.93 (1.28−2.93)	14.6 (12.0−17.8)
46	Me	Bn		>5000 (35%)	>5000 (5%)	>5000 (11%)	2.68 (2.11−3.41)	20.4 (14.3−29.1)
47	Et	Bn		485 (407−578)	>5000 (12%)	>5000 (18%)	2.71 (2.20−3.33)	25.3 (22.7−28.2)

[a] Displacement of specific [^{3}H]DPCPX binding at human A_1 receptors expressed in CHO cells (n = 3−6). [b] Displacement of specific [^{3}H]ZM241385 binding at human A_{2A} receptors expressed in CHO cells (n = 3−6). [c] Potency (IC_{50}) of examined compounds to inhibit 100 nM NECA stimulation cAMP levels in hA_{2B} CHO cells. [d] Displacement of specific [^{3}H]MRE3008F20 binding at human A_3 receptors expressed in CHO cells (n = 3−6). Data are expressed as geometric means with 95% confidence limits. In parentheses are reported the % of inhibition to hA_1, A_{2A}, A_{2B}, and A_3 CHO cells. [e] Potency (IC_{50}) of selected compounds to inhibit 100 nM Cl-IB-MECA inhibition of cAMP levels in hA_3 CHO cells. [f] Not determined.

as condensing agent, followed by ring closure with sodium hydroxide at reflux to afford the desired 3-allyl/benzyl-8-[(substituted)-isoxazol/pyrazol-3/5-yl]-1*H*-purine-2,6(3*H*,7*H*)-dione derivatives (**5a**−**j**).[38] The diamino uracils **4a**,**b** were obtained by reduction of the corresponding nitroso uracils using sodium dithionite.[38]

The substituted pyrazole/isoxazole carboxylic acids were prepared according to procedures reported in literature.[42] The 3-methoxy-isoxazole-5-carboxylic acid was obtained from the reaction of dimethyl acetylenedicarboxylate with hydroxylamine, followed by O-alkylation with methyliodide in presence of K_2CO_3, followed by classical saponification.[43]

The 8-heterocyclyl-xanthine derivatives **5a**−**j** were treated with phosphorus pentasulfide in dry pyridine at reflux to give the corresponding 6-thioxanthine **6a**−**j**. The subsequent reaction with methyliodide in the presence of sodium hydroxide furnished the *S*-methyl-derivatives **7a**−**j** in good yields. Compounds **7a**−**j** were then treated with the appropriate amino alchol (2-amino-butan/propan-1-ol purchased both as racemic mixtures and optically active reagents) in anhydrous DMSO at 150 °C for 1.5 h. Final cyclizations were performed in dichloromethane solution by treatment with thionyl chloride heating at reflux for 18 h. This kind of cyclization is known to yield final compounds with retained stereochemistry.[35]

RESULTS AND DISCUSSION

All the 2-heterocyclyl-imidazo[2,1-*i*]purin-5-one derivatives **28**−**47** (Table 1) were evaluated in radioligand binding assays to determine their affinities for human A_1, A_{2A}, and A_3 adenosine receptors using [^{3}H]-DPCPX (1,3-[3*H*]-dipropyl-8-cyclopentyl-xanthine), [^{3}H]-ZM 241385 (4-(2-[7-amino-2-(2-furyl)[1,2,4]-triazolo[2,3-*a*][1,3,5]triazin-5-ylamino]ethyl)phenol), [^{3}H]-MRE3008F20 (5-*N*-(4-methoxyphenylcarbamoyl)amino-8-propyl-2-(2-furyl)pyrazolo[4,3-*e*]-1,2,4-triazolo[1,5-*c*]pyrimidine), respectively, as radioligands. Efficacy of the compounds versus hA_{2B} AR was investigated, evaluating their capability to inhibit (100 nM) NECA stimulated cAMP production. Antagonism of selected ligands versus hA_3AR was also assessed through cAMP experiments evaluating their capability to block the inhibitory effect mediated by Cl-IB-MECA. Affinity data for A_1, A_{2A}, and A_3 receptors (expressed as K_i values), and IC_{50} values for hA_{2B} and hA_3 subtypes, derived from the cAMP assays, are listed in Table 1.

Structure−Activity Relationships Analysis: hA_3AR Affinity. All the synthesized molecules exhibited high affinities at the hA_3AR subtype with K_i values ranging from 1.46 (compound *R*-**33**) to 44.8 nM (compound **38**). The different kind of heterocycle introduced at the 2-position gave various contributions to the binding profile of the examined imidazo[2,1-*i*]purin-5-one derivatives. The affinities at hA_3AR of 4-allyl-2-(1′,5′-dimethyl-pyrazole) derivatives (**28**, **29**) showed to be about 3- to 4-fold higher than that of the corresponding 4-allyl-2-(1′,3′-dimethyl-pyrazole) isomers (**40**, **41**, respectively), whereas 4-benzyl-2-(1′,5′-dimethyl-pyrazole) derivatives (**30**, **31**) show hA_3 AR K_i binding values similar to those of the corresponding 4-benzyl-2-(1′,5′-dimethyl-pyrazole) derivatives **42** and **43**. This suggests that 1′,5′-disubstitution of the 2-pyrazole ring is equivalent or slightly detrimental, with regard to hA_3 binding affinity, if compared with 1′,3′-disubstitution. The comparison between hA_3 affinities of 2-(1′-methyl-3′-methoxy-pyrazole) derivatives **32**−**35** and 2-(3′-methoxy-isoxazole) derivatives **44**−**47** indicated a substantial bioisosterism of these heterocycles as regards the interaction with hA_3 AR of the examined ligands. As indicated by the affinity values of compounds **28**−**39**, the type of substitutions at the 3′-position of the 2-pyrazole ring appreciably affects the affinity for the hA_3 AR. The order of efficacy OMe (compounds **32**−**35**) > Me (**28**−**31**) > OBn (**36**−**39**) is maintained in the whole subset of molecules. For example, the 3′-OCH_3-derivative **32** (K_i hA_3 = 2.36 nM) appeared 2- and 10-fold more potent in binding hA_3 subtype than the analogously

dx.doi.org/10.1021/jm2004738 |*J. Med. Chem.* 2011, 54, 5205–5220

substituted 3′-CH_3-derivative **28** (K_i hA_3 = 4.56 nM) and 3′-OBn-derivative **36** (K_i hA_3 = 24.7 nM), respectively. Similarly, the 3′-OCH_3-derivative **33** (K_i hA_3 = 1.96 nM) was found to be 1.5- and 11-fold more potent then the corresponding 3′-CH_3 derivative **29** (K_i hA_3 = 3.01 nM) and 3′-OBn derivative **37** (K_i hA_3 = 21.5 nM), respectively, at the hA_3AR. This trend led us to synthesize 3′-OCH_3-isoxazole derivatives **44**−**47**, which confirmed the efficacy of the introducing a methoxy group at the 3′-position of the 2-heterocycle. From the set of molecules we analyzed, it emerged that the kind of substitutions of the 5-membered heterocycle at the 2-position of the imidazo[2,1-*i*]purin-5-one tricycle is particularly important for hA_3 AR binding affinity. A steric control seems to take place around the 3′-position of the 2-heterocycle, as suggested by the decrease of affinities of the 3′-OBn derivatives **36**−**39** (K_i hA_3 ranging from 21.5 to 44.8 nM). Moreover, the angularity component of the 3′-OCH_3, in association with the possibility of this function to establish a hydrogen bond, could contribute to the formation of particular ligand−receptor interactions.

Introduction of a benzyl or an allyl substituent at the 4-position of the imidazo[2,1-*i*]purin-5-one core was also examined. The pairwise comparison between the K_i (hA_3) values of 4-allyl and 4-benzyl derivatives resulted in most cases in preferred affinity for the allyl-substituted compounds (i.e., compounds **30**, **31**, and **35** were 3.8-, 1.6- and 2-fold less potent then the correspondent 4-allyl derivatives **28**, **29**, and **33** as hA_3 ligands). Nevertheless, some exceptions have been observed (see compounds **42**, **43**, and **46** versus **40**, **41**, and **44**, respectively).

The substitution of the 8-position with a methyl or an ethyl seems to be essentially equivalent in terms of hA_3 affinity, as can be deduced from the equipotent binding of the 8-methyl and 8-ethyl derivatives. For example compounds **28** exhibited a binding affinity similar to that of the correspondent 8-ethyl derivative **29**. The same can be observed, for example, for compounds **36**, **38**, and **40** versus **37**, **39**, and **41**, respectively.

The monosubstitution of C^8 generated an asymmetric carbon. For selected compounds (**28**, **31**, **33**, **34**, and **41**), both racemic mixtures and optically active derivatives have been prepared in order to determine if there is a stereoselective preference in the interaction with hA_3 AR. The affinities of racemates at the A_3 AR appeared generally comparable to those of the respective *R* and *S* pure isomers. Only the possibility of a very weak preference for the *R* isomer can be noted (*R*-**28** compared to *S*-**28** or *R*-**33** compared to *S*-**33**). The data related to the 8-position seem to suggest that this side of the molecule may not be involved in forming strong interactions with the hA_3 receptor binding site. In fact, neither the kind of substitution nor the stereoisomeric configuration of C^8 seem to particularly affect the affinity of the ligands for the hA_3 AR.

Structure−Activity Relationships Analysis: hA_3AR vs hA_{2A} and hA_1 ARs Selectivity. Very high levels of hA_3 vs hA_{2A} selectivity have been obtained with all compounds. Indeed, with the exception of derivatives **38** (K_i hA_{2A} = 2010 nM), **39** (K_i hA_{2A} = 2130 nM), and **45** (K_i hA_{2A} = 1520 nM), the K_i values calculated in the binding assay at the hA_{2A} AR were greater than 5 μM. However, the affinity at the hA_1 AR subtype was occasionally considered relevant (lower than 1 μM for compounds **29**, **31**, **35**, and **47**). Comparing the type of heterocycle at the 2-position, the 1,5-disubstituted pyrazole seems to ensure a low affinity at the hA_1 AR. However, derivatives **40**−**43** (K_i hA_1 > 5 μM), displaying from about 330- to 540-fold selectivity for the hA_3 AR over the hA_{2A} AR, are not the most selective of the series because of the concomitant small reduction of hA_3 affinity. The most selective derivatives have been obtained with the introduction of the 2-(1′-methyl-3′-methoxy-pyrazole) or the 2-(3′-methoxy-isoxazole) functions (derivatives **32**−**35** and **44**−**47**, respectively). In particular, compounds **32** (4-allyl-7,8-dihydro-2-(3-methoxy-1-methyl-1*H*-pyrazol-5-yl)-8-methyl-1*H*-imidazo[2,1-*i*]purin-5(4H)-one) and **46** (4-benzyl-8-methyl-7,8-dihydro-2-(3-methoxyisoxazol-5-yl)-1*H*-imidazo[2,1-*i*]purin-5(4*H*)-one) appeared to be the most selective of the series of the 2-heterocyclyl-imidazo[2,1-*i*]purin-5-ones described, displaying more than 2100- and 1800-fold selectivity, respectively, for the hA_3 AR over the other AR subtypes. The kind of substituent at the 3′-position of the 2-(1′,3′-disubstituted-pyrazole) moiety seems to affect the selectivity of the ligands for the hA_3 vs hA_1 AR. In fact, the related affinity ratios (K_i hA_1/K_i hA_3) clearly suggested that the selectivity follows the sequence 3′-OMe > 3′-Me > 3′-OBn. For example, compounds **32** (3′-OMe), **28** (3′-Me), and **36** (3′-OBn) were 2100-, 450-, and 202-fold selective for hA_3 vs hA_1, respectively. The same can be noticed in the comparison of compounds **33** (3′-OMe, K_i hA_1/K_i hA_3 = 780), **29** (3′-Me, K_i hA_1/K_i hA_3 = 170), and **37** (3′-OBn, K_i hA_1/K_i hA_3 = 56) as well as between compounds **34** (K_i hA_1/K_i hA_3 = 610), **30** (K_i hA_1/K_i hA_3 = 291), **38** (K_i hA_1/K_i hA_3 = 57), and derivatives **35** (K_i hA_1/K_i hA_3 = 105), **31** (K_i hA_1/K_i hA_3 = 60), and **39** (K_i hA_1/K_i hA_3 = 42).

In many of the evaluated examples, the 4-allyl substitution provides greater selectivity for K_i hA_1/K_i hA_3 in comparison with 4-benzyl substitution, for example, compounds **32** (K_i hA_1/K_i hA_3 = 2119), which is 3.5-fold more selective then the corresponding 4-benzyl substituted **34** (K_i hA_1/K_i hA_3 = 610). Similarly, the 4-allyl derivative **28** (K_i hA_1/K_i hA_3 = 450) is 1.5-fold more selective for hA_3 vs hA_1 than the corresponding 4-benzyl derivative **30** (K_i hA_1/K_i hA_3 > 290). The only exceptions to this leaning are compounds **40** (K_i hA_1/K_i hA_3 > 359) compared to **42** (K_i hA_1/K_i hA_3 > 400), in which the 4-substitution with a benzyl or an allyl functions seems practically equivalent, and compounds **44** (K_i hA_1/K_i hA_3 > 1397) compared to **46** (K_i hA_1/K_i hA_3 > 1866), in which the effect on hA_3 vs hA_1 selectivity of the two substituents at the 4-position appeared slightly reversed.

While practically equivalent for their effect on hA_3 affinity, the introduction of a methyl or an ethyl at the 8-position appears to influence the affinity of the examined molecules toward the hA_1 AR subtype. The choice of the substituent at this position was therefore important for the optimization of hA_3 over hA_1 selectivity. The general selectivity pattern would quite strongly suggest a preference by A_1 adenosine receptor for the 8-ethyl substitution. This effect is fairly evident if the 8-methyl derivative **46** (K_i hA_1 ≥ 5000, K_i hA_1/K_i hA_3 > 1866) was compared to the 8-ethyl analogue **47** (K_i hA_1 = 485, K_i hA_1/K_i hA_3 = 179). With the exception of compound **43**, the molecules exerting higher affinity at the hA_1 subtype were concomitantly substituted at the 4- and 8-positions with a benzyl and an ethyl moieties, respectively, indicating a synergistic detrimental effect of the two substituents on hA_3 selectivity. On the contrary, the 4-allyl-8-methyl-imidazo[2,1-*i*]purin-5-one derivatives displayed the best K_i hA_1/K_i hA_3 ratios of the series.

A slight level of enantioselectivity seems to concern the interaction of the described ligands with the hA_1 AR subtype. The affinities of the *S* isomers of compounds **28**, **31**, **33**, and **34** were 1.3- to 2.3-fold higher than those of the corresponding *R* isomers, thus resulting in a higher hA_3 vs hA_1 selectivity of the *R*

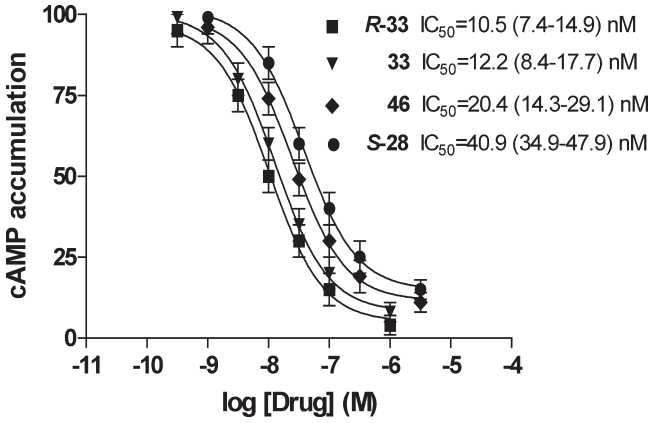

Figure 2. Inhibition curves of cAMP accumulation in hA_3CHO cells by adenosine antagonists blocking the effect of 100 nM Cl-IB-MECA.

isomers with reference to the corresponding *S*-configured molecules. This data resulted in agreement with the findings previously described by Müller and co-workers[35] and appeared to give evidence for a direct involvement of the additional imidazolidine ring in critical interactions between the 2-heterocyclyl-imidazo[2,1-*i*]purinones and the hA_1 AR binding pocket. This could be the reason for the responsiveness of hA_1 AR binding affinities to the kind of substitution and/or the configuration of the C8.

Compound *R*-**33** was found to be the most potent hA_3 AR ligand of the 2-heterocyclyl-imidazo[2,1-*i*]purin-5-one derivatives herein described. It also confirmed to have very high selectivity versus A_{2A}, A_{2B}, and also at A_1 AR, with one of the highest value of K_i hA_1/K_i hA_3 ratio of the series (1729).

Functional Assays: hA_{2B} and hA_3 ARs. All the compounds resulted practically inactive at the hA_{2B} AR subtype (IC_{50} > 5 μM, see Table 1).

The tested compounds confirmed to operate as antagonists of the hA_3 AR subtype in the cAMP functional assay. Interestingly, a good accordance between binding and functional experiments performed with hA_3 receptor has been revealed. The molecules showing the best affinities for hA_3 adenosine receptor have also proved to have very high potency (IC_{50} values in the low nanomolar range) in the functional assay (Figure 2, Table 1). Derivative *R*-**33**, showing the highest hA_3 affinity, also emerged as the most potent compound of the series with an IC_{50} value of 10.5 nM.

Molecular Modeling Studies. Molecular modeling studies were performed with the aim of rationalizing the aforementioned SAR data both in terms of affinity for the hA_3 AR and selectivity of binding for this receptor versus the hA_1 and hA_{2A} ARs. To this end, the recently published crystal structure of the hA_{2A} receptor (PDB code 3EML)[44] in complex with compound ZM241385 was used to obtain a homology model of the hA_1 and hA_3 ARs. The sequence alignment between the three receptors as well as the positions of the disulfide bridges were attained consistently with what was already suggested by Moro and co-workers.[45] The structures of the modeled receptors were used to perform docking calculations of the most potent and selective compound *R*-**33** employing the Glide program of the Schrodinger package that was already used to successfully dock a series of ARs antagonists.[46] The docking poses obtained were evaluated for their consistency with the available SAR data as well as for the Glide scores obtained from these calculations.

Docking calculations obtained for *R*-**33** in complex with hA_3 AR revealed that in the best Glide score (−6.75), the ligand binds to the outer portion of the A_3 AR being surrounded by TMs 3, 5, 6,7 helices and EL2 (Figure 3). In this position, the imidazo[2,1-*i*]purin-5-one scaffold establishes a π-stacking interaction with F168 and a H-bond between its N^3 atom and N250 side chain. Interestingly, the latter residue was found to be critical for ligand binding at both the A_3 and A_{2A} ARs.[47,48]

In addition, the 4-allyl substituent points toward the outer part of the receptor taking favorable hydrophobic contacts with V169, M174, M177, and I253 (herein referred as L1 pocket). Docking calculations on compound **35** (see Figure S1 in Supporting Information) indicated that while the imidazo[2,1-*i*]purin-5-one scaffold occupies the same position in the hA_3 AR, now the bulky 4-benzyl substituent points outward being less prone to efficiently occupy the L1 cleft. This might explain why compounds featuring a 4-allyl substituent are generally characterized by a higher affinity at the hA_3 receptor if compared with the corresponding 4-benzyl compounds.

In the same calculated binding pose, the *R*-**33** 8-ethyl group points toward transmembrane helices 2 and 3, although this substituent is too distant from this region of the receptor to play a critical role in the receptor binding. This result is in accordance with SAR data indicating that the substitution of the 8-position with a methyl or an ethyl and the inversion of the chiral C^8 does not significantly affect the binding at the hA_3 AR, these data were further confirmed by docking results achieved for compound *S*-**33** (see Figure S2 in Supporting Information).

If compared with the 8-ethyl group, the 1′-methyl-3′-methoxy-pyrazole ring in the 2-position is able to make favorable hydrophobic contact with the receptor, being embedded in a rather profound pocket (herein referred as L2) made up by L91, M177, I186, W243, L246, and S247. Here, the 3′-methoxy accepts an H-bond from the latter residue and the interaction with W243 should be considered to be responsible for the antagonist properties of this ligand, as already demonstrated for other AR antagonists.[47] Also in this case, the position of the pendant ring in position 2- in the A_3 AR seems to explain the SAR data achieved for this portion of the molecule. Indeed, as indicated above, the substitution of the methoxy group with a methyl one (compounds *R*-**28**, *S*-**28**, **29**, **30**, *R*-**31**, and *S*-**31**) leads to a decrease of affinity due to the loss of a H-bond with S247 (see Figure S3 in Supporting Information), while a further decrease of affinity is recorded for the bulkier benzyloxy derivatives that are less easily hosted in the L2 pocket (compounds **36**−**39**).

Docking results were also helpful in rationalizing the lower affinity at the A_3AR of compounds **40**−**43**. In fact, when docking *R*-**41** in the A_3AR, the resulting binding pose was similar to the one predicted for *R*-**33** (see Figure S4 in Supporting Information), nevertheless the presence of two methyl groups on the pendant pyrazole ring results in the loss of the H-bond interaction with S247. On the other hand, replacement of the pendant 1′-methyl-3′-methoxy-pyrazole ring with the 3′-methoxy-isoxazole one (compounds **44**−**47**) still allows the aforementioned interaction with the receptor (see Figure S5 in Supporting Information) explaining why the two series display the same binding and selectivity properties at the ARs.

R-**33** was predicted to bind at the hA_1 and hA_{2A} AR structures in a different fashion if compared with the calculated *R*-**33**/hA_3 AR complex (Figure 4). In fact, in the best scoring pose (Glide scores of −5.43 and −5.81 for hA_1 and hA_{2A} ARs, respectively), the 8-ethyl group of the ligand points toward outer part of the

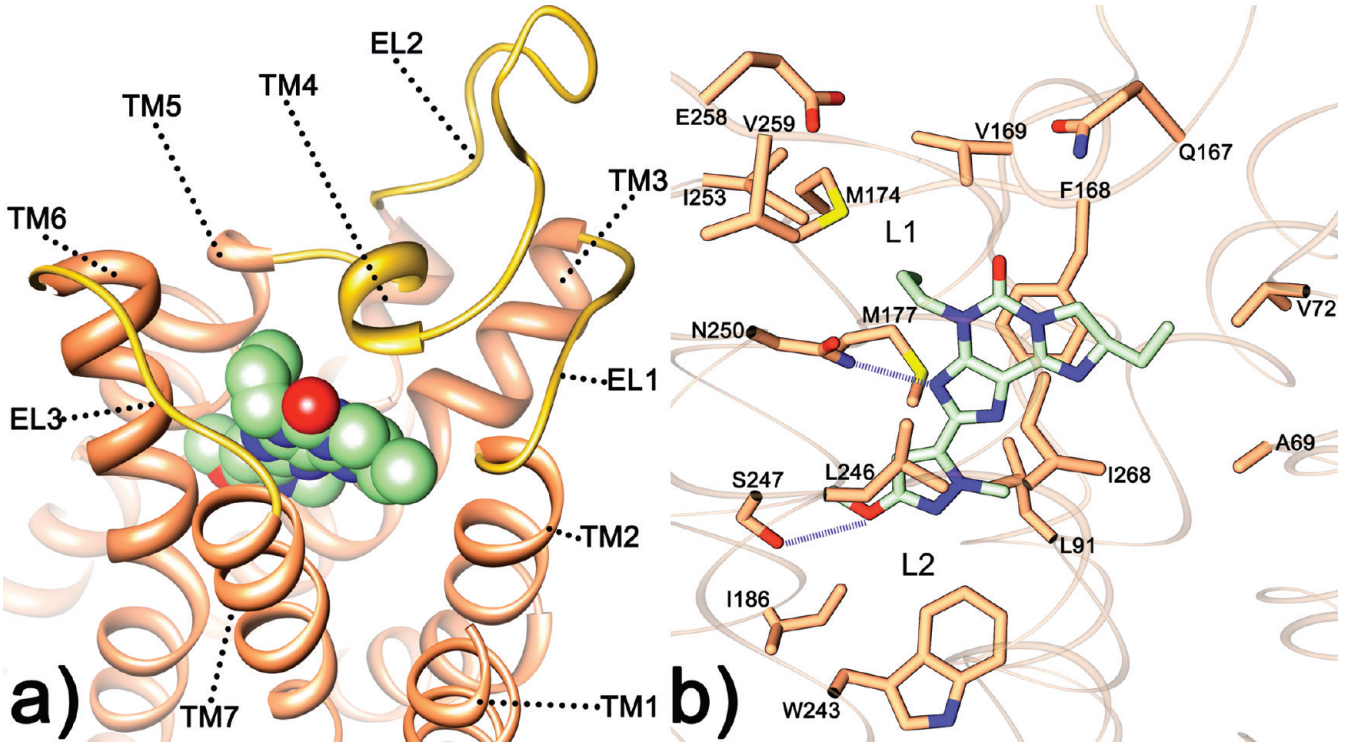

Figure 3. (a) View of the *R*-**33**/hA_3 AR complex. (b) Close view of the calculated binding pose for *R*-**33** in the hA_3 AR mode.

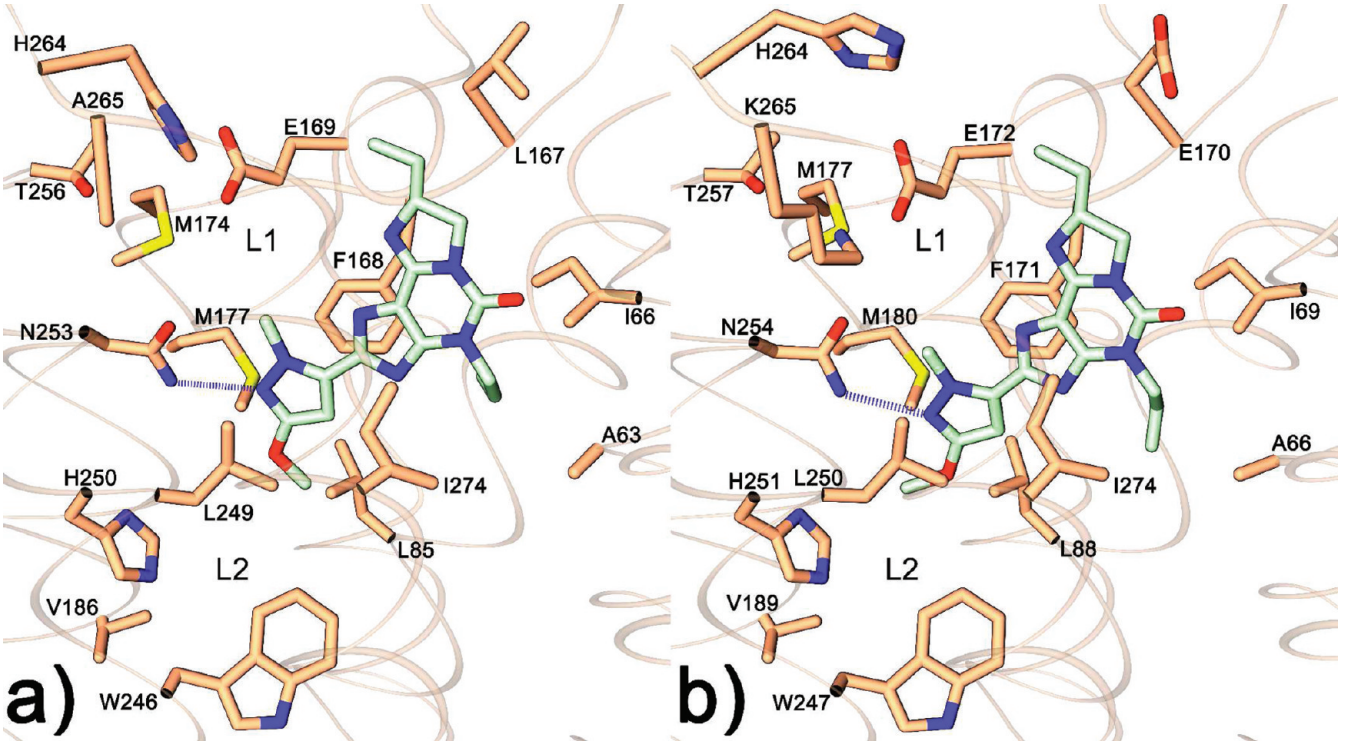

Figure 4. Close-up view of the calculated binding pose for *R*-**33** in the hA_1 AR (a) and hA_{2A} AR structures.

receptors, while the 4-allyl substituent is in the vicinity of the TM2 and TM3 helices. In this position, the critical N254 (hA_1) and N253 (hA_{2A}) residues are H-bonded by the 2′ nitrogen of the 1′-methyl-3′-methoxy-pyrazole ring, while F171 (hA_1) and F168 (hA_{2A}) residues are in contact with the imidazo-[2,1-*i*]purin-5-one core through a π-stacking interaction.

dx.doi.org/10.1021/jm2004738 |*J. Med. Chem.* 2011, 54, 5205–5220

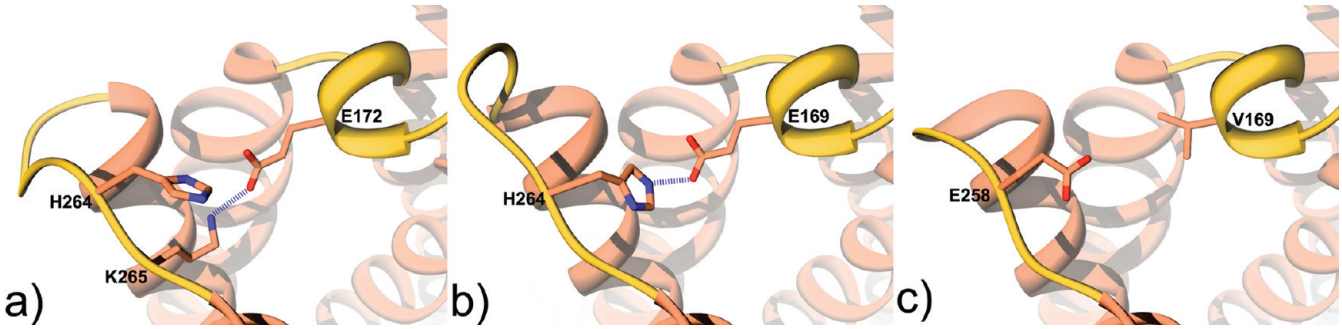

Figure 5. Close-up view of some important residues of the L1 pocket in the hA_1 (a), hA_{2A} and hA_3 ARs.

A comparison of the *R*-**33**/hA_3 with the *R*-**33**/hA_1 and *R*-**33**/hA_{2A} complexes reveals that, for the latter complexes, both the L1 and L2 pockets are not efficiently contacted by the ligand. This behavior should be ascribed to the different amino acid composition of the L1 pocket. Indeed, in the hA_1 and hA_{2A} AR respectively, the E172 and E169 residues belonging to the EL2 region are replaced by V169 in the hA_3 AR, resulting in different electrostatic properties of the L1 cleft. Moreover, the presence of a glutamate residue makes this cleft narrower and less prone to be occupied be the ligand substituents. In principle, it may be argued that the flexible EL2 domain could undergo a conformational rearrangement to allow the opening of the L1 pocket in hA_1 and hA_{2A} ARs. Nevertheless, such an event seems unlikely to happen given that in the hA_{2A} AR, the conformation of E169 is stabilized by an electrostatic interaction with H264 in EL3. The same holds true for E172 in hA_1, which is involved in the same sort of interaction with K265 (Figure 5). In this respect, the position of H264 seems to be relatively constrained, as demonstrated experimentally by Stevens and co-workers.[44] Similar results were also recently achieved by Moro and co-workers, postulating the different residue composition of the L1 pocket should influence not only the binding pose but also the access of the ligands to the TM region of the receptors.[45]

Thus, the different residue composition of the L1 pocket also prevents the ligand to make contacts with the L2 cleft in which a tryptophan residue (W243, W247, and W246 in the hA_3, hA_1, and hA_{2A} ARs, respectively) is believed to play a crucial role in receptor activation and in antagonist binding.[47] This should explain why the great majority of the 2-heterocyclyl-imidazo[2,1-*i*]purin-5-ones described herein are endowed with high binding selectivity toward the hA_3 AR.

CONCLUSIONS

In conclusion, a new series of 2-heterocyclyl-imidazo[2,1-*i*]purin-5-one derivatives has been synthesized and tested at the four known ARs. The 2-heterocyclyl substitution proved to induced excellent affinity and selectivity toward hA_3 AR subtype. Molecular modeling studies were helpful in rationalizing the observed structure−activity relationships along with the selectivity profiles of the new series of ligands. Docking of the most potent compound (*R*-**33**) in complex with hA_3 AR furnished a general survey of the hypothetical binding mode of the newly described derivatives. The A_3 AR antagonists herein described, standing out for their remarkable potency and selectivity, will be further investigated to clarify their potential for future drug development and clinical application.

EXPERIMENTAL SECTION

Chemistry. Reaction progress and product mixtures were monitored by thin-layer chromatography (TLC) on silica gel (precoated F254 Merck plates) and visualized with aqueous potassium permanganate. ^{1}H NMR data were determined in $CDCl_3$ or DMSO-d_6 solutions with a Varian VXR 200 spectrometer or a Varian Mercury Plus 400 spectrometer. Peak positions are given in parts per million (δ) downfield from tetramethylsilane as internal standard, and *J* values are given in hertz. Light petroleum refers to the fractions boiling at 40−60 °C. Melting points were determined on a Buchi−Tottoli instrument and are uncorrected. Chromatography was performed on Merck 230−400 mesh silica gel. Organic solutions were dried over anhydrous sodium sulfate. Elemental analyses were performed by the microanalytical laboratory of Dipartimento di Chimica, Università di Ferrara, and were within ±0.4% of the theoretical values for C, H, and N. All final compounds revealed a purity of not less than 95%. The mass spectra were obtained on a ESI Micromass ZMD 2000 mass spectrometer. Chiral amino alcohols were purchased from Alfa Aesar or Aldrich in the highest available purity grade.

General Procedure for the Synthesis of 3-Allyl/benzyl-8-[(substituted)isoxazol/pyrazol-3/5-yl]-1*H*-purine-2,6(3*H*,7*H*)-dione Derivatives (5a−j). To a solution of the appropriately substituted isoxazole/pyrazole-carboxylic acid (2.5 mmol) in DMF (7 mL), EDAC·HCl (2.5 mmol, *N*-ethyl-*N*′-(3-dimethylaminopropyl)carbodiimide hydrochloride) and HOBt (2.5 mmol, hydroxybenzotriazole) were added. The mixture was stirred at room temperature for 10 min, and then 5,6-diamino-1-allyl/benzyl-1*H*-pyrimidine-2,4-dione (2.5 mmol) was added. The mixture was stirred for further 24 h, and then the solvent was evaporated and the residue was suspended with H_2O (30 mL) to favor the precipitation of a solid, which was subsequently filtered and washed with cold H_2O. The solid was suspended with a 10% aqueous solution of NaOH, and the mixture was refluxed for 1.5 h. The reaction was cooled to 0 °C and acidified with a 10% aqueous solution of HCl to obtain a white precipitate, which was filtered, washed with cold water, and finally crystallized from DMF−H_2O.

3-Allyl-8-(1,3-dimethyl-1H-pyrazol-5-yl)-1H-purine-2,6(3H,7H)-dione (***5a***). Pale-white solid; 65% yield; mp >300 °C. ^{1}H NMR (200 MHz, DMSO-d_6) δ ppm 13.83 (bs, 1H), 11.24 (bs, 1H), 6.77 (s, 1H), 5.97−5.88 (m, 1H), 5.22−5.14 (m, 2H), 4.56 (m, 2H), 4.11 (s, 3H), 2.18 (s, 3H).

3-Benzyl-8-(1,3-dimethyl-1H-pyrazol-5-yl)-1H-purine-2,6(3H,7H)-dione (***5b***). White solid; 57% yield; mp >300 °C. ^{1}H NMR (200 MHz, DMSO-d_6) δ ppm 13.90 (bs, 1H), 11.25 (s, 1H), 7.32 (m, 5H), 6.75 (s, 1H), 5.15 (s, 2H), 4.10 (s, 3H), 2.17 (s, 3H).

3-Allyl-8-(3-methoxy-1-methyl-1H-pyrazol-5-yl)-1H-purine-2,6(3H,7H)-dione (***5c***). White solid; 81% yield; mp >300 °C. ^{1}H NMR (200 MHz, DMSO-d_6) δ ppm 13.93 (bs, 1H), 11.27 (s, 1H), 6.45 (s, 1H), 6.11−5.92 (m, 1H), 5.22−5.13 (m, 2H), 4.57 (d, *J* = 5 Hz, 2H), 4.06 (s, 3H), 3.79 (s, 3H).

*3-Benzyl-8-(3-methoxy-1-methyl-1H-pyrazol-5-yl)-1H-purine-2,6-(3H,7H)-dione (**5d**).* White solid; 60% yield; mp >300 °C. ^{1}H NMR (200 MHz, DMSO-d_6) δ ppm 13.89 (bs, 1H), 11.32 (s, 1H), 7.43−7.22 (m, 5H), 6.41 (s, 1H), 5.15 (s, 2H), 4.05 (s, 3H), 3.79 (s, 3H).

*3-Allyl-8-(3-(benzyloxy)-1-methyl-1H-pyrazol-5-yl)-1H-purine-2,6-(3H,7H)-dione (**5e**).* White solid; 57% yield; mp 296 °C dec. ^{1}H NMR (200 MHz, DMSO-d_6) δ ppm 13.87 (bs, 1H), 11.27 (s, 1H), 7.43−7.36 (m, 5H), 6.46 (s, 1H), 6.02−5.87 (m, 1H), 5.16−5.13 (m, 4H), 4.57 (d, J = 5 Hz, 2H), 4.07 (s, 3H).

*3-Benzyl-8-(3-(benzyloxy)-1-methyl-1H-pyrazol-5-yl)-1H-purine-2,6(3H,7H)-dione (**5f**).* White solid; 58% yield; mp >300 °C. ^{1}H NMR (200 MHz, DMSO-d_6) δ ppm 13.94 (bs, 1H), 11.32 (s, 1H), 7.43−7.29 (m, 10H), 6.45 (s, 1H), 5.16 (s, 4H), 4.06 (s, 3H).

*3-Allyl-8-(1,5-dimethyl-1H-pyrazol-3-yl)-1H-purine-2,6(3H,7H)-dione (**5g**).* White solid; 66% yield; mp >300 °C. ^{1}H NMR (200 MHz, DMSO-d_6) δ ppm 13.61 (bs, 1H), 11.08 (s, 1H), 6.65 (s, 1H), 5.87 (m, 1H), 5.15−5.04 (m, 2H), 4.56 (m, 2H), 3.80 (s, 3H), 2.29 (s, 3H).

*3-Benzyl-8-(1,5-dimethyl-1H-pyrazol-3-yl)-1H-purine-2,6(3H,7H)-dione (**5h**).* White solid; 77% yield; mp >300 °C. ^{1}H NMR (200 MHz, DMSO-d_6) δ ppm 13.45 (bs, 1H), 11.14 (s, 1H), 7.33−7.10 (m, 5H), 6.65 (s, 1H), 5.15 (s, 2H), 3.79 (s, 3H), 2.29 (s, 3H).

*3-Allyl-8-(3-methoxyisoxazol-5-yl)-1H-purine-2,6(3H,7H)-dione (**5i**).* Pale-white solid; 45% yield; mp 297 °C. ^{1}H NMR (200 MHz, DMSO-d_6) δ ppm 14.55 (bs, 1H), 11.37 (s, 1H), 6.84 (s, 1H), 6.01−5.87 (m, 1H), 5.16−5.06 (m, 2H), 4.56 (m, 2H), 3.96 (s, 3H).

*3-Benzyl-8-(3-methoxyisoxazol-5-yl)-1H-purine-2,6(3H,7H)-dione (**5j**).* Pale-yellow solid; 40% yield; mp 284 °C dec. ^{1}H NMR (200 MHz, DMSO-d_6) δ ppm 14.45 (bs, 1H),11.41 (bs, 1H), 7.34−7.22 (m, 5H), 6.84 (s, 1H), 5.15 (s, 2H), 3.96 (s, 3H).

General Procedure for the Synthesis of 3-Allyl/benzyl-1,6-dihydro-8-[(substituted)isoxazol/pyrazol-3/5-yl]-6-thioxo-3*H*-purin-2(7*H*)-one derivatives (6a−j).[35] The appropriate 3-allyl/benzyl-8-[(substituted)isoxazol/pyrazol-3/5-yl]-1*H*-purine-2,6(3*H*,7*H*)-dione derivative **5a−j** (1.5 mmol) was dissolved with pyridine (10 mL), and 2.55 mmol of P_2S_5 were added. The reaction was vigorously stirred at 140 °C for 5 h and then cooled at 0 °C. After the addition of water (30 mL), a pale-green solid precipitated, which was filtered, washed with cold water, and crystallized from DMF/H_2O.

*3-Allyl-1,6-dihydro-8-(1,3-dimethyl-1H-pyrazol-5-yl)-6-thioxo-3H-purin-2(7H)-one (**6a**).* Pale-yellow solid; 95% yield; mp 272 °C. ^{1}H NMR (200 MHz, DMSO-d_6) δ ppm 13.80 (bs, 1H), 12.40 (s, 1H), 7.01 (s, 1H), 6.10−5.80 (m, 1H), 5.25−5.16 (m, 2H), 4.59 (d, 2H, J = 5.8), 4.12 (s, 3H), 2.19 (s, 3H).

*3-Benzyl-1,6-dihydro-8-(1,3-dimethyl-1H-pyrazol-5-yl)-6-thioxo-3H-purin-2(7H)-one (**6b**).* Yellow solid; 87% yield; mp 265 °C. ^{1}H NMR (200 MHz, DMSO-d_6) δ ppm 13.66 (bs, 1H), 12.28 (bs, 1H), 7.32 (m, 5H), 6.86 (s, 1H), 5.17 (s, 2H), 3.81 (s, 3H), 2.30 (s, 3H).

*3-Allyl-1,6-dihydro-8-(3-methoxy-1-methyl-1H-pyrazol-5-yl)-6-thioxo-3H-purin-2(7H)-one (**6c**).* Pale-yellow; 82% yield; mp 272 °C dec. ^{1}H NMR (200 MHz, DMSO-d_6) δ ppm 13.81 (bs, 1H), 12.43 (bs, 1H), 6.68 (s, 1H), 6.11−5.97 (m, 1H), 5.25−5.16 (m, 2H), 4.60 (d, J = 4.6 Hz, 2 H), 4.07 (s, 3H), 3.80 (s, 3H).

*3-Benzyl-1,6-dihydro-8-(3-methoxy-1-methyl-1H-pyrazol-5-yl)-6-thioxo-3H-purin-2(7H)-one (**6d**).* Pale-yellow solid; 84% yield; mp 293−295 °C. ^{1}H NMR (200 MHz, DMSO-d_6) δ ppm 13.92 (bs, 1H), 12.48 (bs, 1H), 7.40−7.30 (m, 5H), 6.68 (s, 1H), 5.18 (s, 2H), 4.06 (s, 3H), 3.80 (s, 3H).

*3-Allyl-8-(3-(benzyloxy)-1-methyl-1H-pyrazol-5-yl)-1,6-dihydro-6-thioxo-3H-purin-2(7H)-one (**6e**).* Pale-yellow solid; 71% yield; mp 241 °C dec. ^{1}H NMR (200 MHz, DMSO-d_6) δ ppm 13.82 (bs, 1H), 12.43 (bs, 1H), 7.44−7.36 (m, 5H), 6.71 (s, 1H), 6.15−5.82 (m, 1H), 5.25−5.16 (m, 2H), 4.60 (d, J = 4 Hz, 2H), 4.08 (s, 3H).

*3-Benzyl-8-(3-(benzyloxy)-1-methyl-1H-pyrazol-5-yl)-1,6-dihydro-6-thioxo-3H-purin-2(7H)-one (**6f**).* Pale-yellow solid; 96% yield; mp 244 °C. ^{1}H NMR (200 MHz, DMSO-d_6) δ ppm 13.89 (bs, 1H), 12.50 (s, 1H), 7.47−7.30 (m, 10H), 6.72 (s, 1H), 5.19 (s, 2H), 5.17 (s, 2H), 4.08 (s, 3H).

*3-Allyl-1,6-dihydro-8-(1,5-dimethyl-1H-pyrazol-3-yl)-6-thioxo-3H-purin-2(7H)-one (**6g**).* Yellow solid; yield 83%; mp 280−282 °C. ^{1}H NMR (200 MHz, DMSO-d_6) δ ppm 13.60 (bs, 1H), 12.23 (bs, 1H), 6.86 (s, 1H), 5.97−5.89 (m, 1H), 5.18−5.06 (m, 2H), 4.58 (d, J = 4.6 Hz, 2H), 3.82 (s, 3H), 2.31 (s, 3H).

*3-Benzyl-1,6-dihydro-8-(1,5-dimethyl-1H-pyrazol-3-yl)-6-thioxo-3H-purin-2(7H)-one (**6h**).* Yellow solid; yield 87%; mp 288 °C. ^{1}H NMR (200 MHz, DMSO-d_6) δ ppm 13.63 (bs, 1H), 12.26 (bs, 1H), 7.30 (m, 5H), 6.84 (s, 1H), 5.15 (s, 2H), 3.78 (s, 3H), 2.28 (s, 3H).

*3-Allyl-1,6-dihydro-8-(3-methoxyisoxazol-5-yl)-6-thioxo-3H-purin-2(7H)-one (**6i**).* Pale-yellow solid; 75% yield; mp 254 °C dec. ^{1}H NMR (200 MHz, DMSO-d_6) δ ppm 14.51 (bs, 1H), 12.61 (bs, 1H), 8.63 (s, 1H), 6.12−5.82 (m, 1H), 5.21 (m, 2H), 4.62 (m, 2H), 4.02 (s, 3H).

*3-Benzyl-1,6-dihydro-8-(3-methoxyisoxazol-5-yl)-6-thioxo-3H-purin-2(7H)-one (**6j**).* Pale-green solid; 96% yield; mp 205 °C dec. ^{1}H NMR (200 MHz, DMSO-d_6) δ ppm 14.45 (bs, 1H), 12.62 (bs, 1H), 8.59 (s, 1H), 7.43−7.19 (m, 5H), 5.17 (s, 2H), 3.97 (s, 3H).

General Procedure for the Synthesis of 3-Allyl/benzyl-8-[(substituted)isoxazol/pyrazol-3/5-yl]-6-(methylthio)-3*H*-purin-2(7*H*)-one Derivatives (7a−j). The appropriate 3-allyl/benzyl-1,6-dihydro-8-[(substituted)isoxazol/pyrazol-3/5-yl]-6-thioxo-3*H*-purin-2(7*H*)-one derivative **6a−j** (1 mmol) was dissolved in 10 mL of NaOH 0.5 N and EtOH (5 mL). After cooling at 0 °C, CH_3I (1.5 mmol) was added and the reaction was stirred at room temperature for 3 h. The mixture was acidified with HCl 5% to obtain a precipitate, which was collected by filtration, washed with cold H_2O, and dried under vacuum.

*3-Allyl-8-(1,3-dimethyl-1H-pyrazol-5-yl)-6-(methylthio)-3H-purin-2(7H)-one (**7a**).* Pale-white solid; 68% yield; mp 250−252 °C. ^{1}H NMR (200 MHz, DMSO-d_6) δ ppm 13.63 (bs, 1H), 6.82 (s 1H), 6.17−5.85 (m, 1H), 5.19 (m, 2H), 4.68 (d, J = 5.2 Hz, 2H), 4.14 (s, 3H), 2.63 (s, 3H), 2.21 (s, 3H).

*3-Benzyl-8-(1,3-dimethyl-1H-pyrazol-5-yl)-6-(methylthio)-3H-purin-2(7H)-one (**7b**).* Yellow solid; 93% yield; mp 163−165 °C. ^{1}H NMR (200 MHz, DMSO-d_6) δ ppm 13.76 (bs, 1H), 7.30−7.26 (m, 5H), 6.69 (s, 1H), 5.25 (s, 2H), 3.83 (s, 3H), 2.56 (s, 3H), 2.32 (s, 3H).

*3-Allyl-8-(3-methoxy-1-methyl-1H-pyrazol-5-yl)-6-(methylthio)-3H-purin-2(7H)-one (**7c**).* Pale-yellow solid; 78% yield; mp 243 °C dec. ^{1}H NMR (200 MHz, DMSO-d_6) δ ppm 13.63 (bs, 1H), 6.39 (s, 1H), 6.15−5.86 (m, 1H), 5.17−5.11 (m, 2H), 4.66 (d, J = 4.8 Hz, 2H), 4.07 (s, 3H), 3.80 (s, 3H), 2.62 (s, 3H).

*3-Benzyl-8-(3-methoxy-1-methyl-1H-pyrazol-5-yl)-6-(methylthio)-3H-purin-2(7H)-one (**7d**).* White solid; 48% yield; mp 268−270 °C. ^{1}H NMR (200 MHz, DMSO-d_6) δ ppm 13.73 (bs, 1H), 7.39−7.27 (m, 5H), 6.46 (s, 1H), 5.25 (s, 2H), 4.08 (s, 3H), 3.81 (s, 3H), 2.63 (s, 3H).

*3-Allyl-8-(3-(benzyloxy)-1-methyl-1H-pyrazol-5-yl)-6-(methylthio)-3H-purin-2(7H)-one (**7e**).* Pale-yellow solid; 85% yield; mp 224 °C. ^{1}H NMR (200 MHz, DMSO-d_6) δ ppm 13.79 (bs, 1H), 7.4−7.34 (m, 5H), 6.53 (s, 1H), 6.15−5.87 (m, 1H), 5.19−5.11 (m, 4H), 4.68 (d, J = 4.4 Hz, 2H), 4.09 (s, 3H), 2.62 (s, 3H).

*3-Benzyl-8-(3-(benzyloxy)-1-methyl-1H-pyrazol-5-yl)-6-(methylthio)-3H-purin-2(7H)-one (**7f**).* White solid; 87% yield; mp 228 °C. ^{1}H NMR (200 MHz, DMSO-d_6) δ ppm 13.79 (bs, 1H), 7.43−7.27 (m, 5H), 6.47 (s, 1H), 5.26 (s, 2H), 5.18 (s, 2H), 4.10 (s, 3H), 2.63 (s, 3H).

*3-Allyl-8-(1,5-dimethyl-1H-pyrazol-3-yl)-6-(methylthio)-3H-purin-2(7H)-one (**7g**).* White solid; 95% yield; mp 242−244 °C. ^{1}H NMR (200 MHz, DMSO-d_6) δ ppm 13.99 (bs, 1H), 6.71 (s, 1H), 6.11−5.85 (m, 1H), 5.16−5.03 (m, 2H), 4.67 (d, J = 4.6 Hz, 2H), 3.84 (s, 3H), 2.61 (s, 3H), 2.32 (s, 3H).

*3-Allyl-8-(1,5-dimethyl-1H-pyrazol-3-yl)-6-(methylthio)-3H-purin-2(7H)-one (**7h**).* White solid; 82% yield; mp 183 °C. ^{1}H NMR (200

MHz, DMSO-d_6) δ ppm 13.80 (bs, 1H), 7.30 (m, 5H), 6.69 (s, 1H), 5.25 (s, 2H), 3.83 (s, 3H), 2.56 (s, 3H), 2.31 (s, 3H).

*3-Allyl-8-(3-methoxyisoxazol-5-yl)-6-(methylthio)-3H-purin-2(7H)-one (**7i**).* Pale-yellow solid; 73% yield; mp 271 °C dec. ^{1}H NMR (200 MHz, DMSO-d_6) δ ppm 14.38 (bs, 1H), 6.90 (s, 1H), 6.09−5.80 (m, 1H), 5.11 (m, 2H), 4.65 (m, 2H), 3.97 (s, 3H), 2.67 (s, 3H).

*3-Benzyl-8-(3-methoxyisoxazol-5-yl)-6-(methylthio)-3H-purin-2(7H)-one (**7j**).* Pale-yellow solid; 75% yield; mp 249−251 °C dec. ^{1}H NMR (200 MHz, DMSO-d_6) δ ppm 14.62 (bs, 1H), 7.35−7.28 (m, 5H), 6.91 (s, 1H), 5.25 (s, 2H), 3.97 (s, 3H), 2.68 (s, 3H).

General Procedure for the Synthesis of 6-(1-Hydroxybutan/propan-2-ylamino)-3-allyl/benzyl-8-[(substituted)isoxazol/pyrazol-3/5-yl]-3*H*-purin-2(7*H*)-one Derivatives (8−27). The appropriate 3-allyl/benzyl-8-[(substituted)isoxazol/pyrazol-3/5-yl]-6-(methylthio)-3*H*-purin-2(7*H*)-one derivative **7a**−**j** (0.3 mmol) was suspended in anhydrous DMSO (0.3 mL) and, after cooling at 0 °C, the opportune (*R*/*S*/*R*,*S*)-2-amino-butan/propan-1-ol (1.5 mmol) was added. The reaction was heated at 150 °C for 1 h. The solvent was evaporated under vacuum and the product was precipitated from CH_2Cl_2−Et_2O, filtered, washed with Et_2O, and finally purified by column chromatography on silica gel eluting with EtOAc/CH_3OH 9.5:0.5.

*(R,S)-6-(1-Hydroxypropan-2-ylamino)-3-allyl-8-(1,3-dimethyl-1H-pyrazol-5-yl)-3H-purin-2(7H)-one (**8**).* White solid; 56% yield; mp 255−256 °C. ^{1}H NMR (200 MHz, DMSO-d_6) δ ppm 12.98 (bs, 1H), 7.43 (bs, 1H), 6.45 (s, 1H), 6.18−5.83 (m, 1H), 5.18−5.03 (m, 3H), 4.59 (d, J = 3 Hz, 2H), 4.22 (m, 1H), 4.13 (s, 3H), 3.58 (m, 2H), 2.18 (s, 3H), 1.22 (m, 3H). MS (ESI): $[MH]^+$ = 344.3.

*(R)-6-(1-Hydroxypropan-2-ylamino)-3-allyl-8-(1,3-dimethyl-1H-pyrazol-5-yl)-3H-purin-2(7H)-one (R-**8**).* White solid; 66% yield; mp dec 253−254 °C. ^{1}H NMR (200 MHz, DMSO-d_6) δ ppm 12.38 (bs, 1H), 7.43 (bs, 1H), 6.45 (s, 1H), 6.03−5.84 (m, 1H), 5.14−5.08 (m, 3H), 4.57 (d, J = 4.8 Hz, 2H), 4.21 (m, 1H), 4.11 (s, 3H), 3.51 (m, 2H), 2.17 (s, 3H), 1.22−1.16 (m, 3H). MS (ESI): $[MH]^+$ = 344.3.

*(S)-6-(1-Hydroxypropan-2-ylamino)-3-allyl-8-(1,3-dimethyl-1H-pyrazol-5-yl)-3H-purin-2(7H)-one (S-**8**).* White solid; 52% yield; mp dec 253−254 °C. ^{1}H NMR (200 MHz, DMSO-d_6) δ ppm 12.80 (bs, 1H), 7.42 (bs, 1H), 6.48 (s, 1H), 6.05−5.82 (m, 1H), 5.15−4.92 (m, 3H), 4.58 (d, J = 5.0 Hz, 2H), 4.22 (m, 1H), 4.12 (s, 3H), 3.51 (m, 2H), 2.19 (s, 3H), 1.22−1.17 (m, 3H). MS (ESI): $[MH]^+$ = 344.3.

*(R,S)-6-(1-Hydroxybutan-2-ylamino)-3-allyl-8-(1,3-dimethyl-1H-pyrazol-5-yl)-3H-purin-2(7H)-one (**9**).* White solid; 62% yield; mp dec 253−255 °C. ^{1}H NMR (200 MHz, DMSO-d_6) δ ppm 12.47 (bs, 1H), 7.52 (bs, 1H), 6.45 (s, 1H), 6.10−5.85 (m, 1H), 5.20−5.10 (m, 2H), 5.00−4.80 (bs, 1H), 4.57 (d, J = 4.6 Hz, 2H), 4.12 (m, 4H), 4.75−4.67 (m, 2H), 2.16 (m, 3H), 1.80−1.60 (m, 2H), 1.12−0.80 (m, 3H). MS (ESI): $[MH]^+$ = 357.5.

*(R,S)-6-(1-Hydroxypropan-2-ylamino)-3-benzyl-8-(1,3-dimethyl-1H-pyrazol-5-yl)-3H-purin-2(7H)-one (**10**).* White solid; 46% yield; mp 230−233 °C. ^{1}H NMR (200 MHz, DMSO-d_6) δ ppm 12.70 (bs, 1H), 7.31−7.20 (m, 6H), 6.55 (s, 1H), 5.14 (s, 2H), 4.95 (bs, 1H), 4.19 (m, 1H), 3.82 (s, 3H), 3.47 (m, 2H), 2.30 (s, 3H), 1.18 (d, 3H, J = 6.6 Hz). MS (ESI): $[MH]^+$ = 394.5.

*(R,S)-6-(1-Hydroxybutan-2-ylamino)-3-benzyl-8-(1,3-dimethyl-1H-pyrazol-5-yl)-3H-purin-2(7H)-one (**11**).* White solid; 72% yield; mp 171−172 °C. ^{1}H NMR (200 MHz, DMSO-d_6) δ ppm 12.65 (bs, 1H), 7.40−7.26 (m, 6H), 6.56 (s, 1H), 5.16 (s, 2H), 4.89−4.81 (m, 1H), 4.12 (m, 4H), 3.60−3.40 (m, 2H), 2.19−2.15 (m, 3H), 1.80−1.67 (m, 2H), 0.87 (t, J = 7.2 Hz, 3H). MS (ESI): $[MH]^+$ = 408.2.

*(R)-6-(1-Hydroxybutan-2-ylamino)-3-benzyl-8-(1,3-dimethyl-1H-pyrazol-5-yl)-3H-purin-2(7H)-one (R-**11**).* White solid; 45% yield; mp 170−172 °C. ^{1}H NMR (400 MHz, DMSO-d_6) δ ppm 12.70 (bs, 1H), 7.31−7.26 (m, 6H), 6.56 (s, 1H), 5.16 (s, 2H), 4.88−4.79 (m, 1H), 4.06−4.04 (m, 1H), 3.82 (s, 3H), 3.532−3.43 (m, 1H), 2.31 (s, 3H), 1.69−1.67 (m, 1H), 1.52−1.49 (m, 1H), 0.92 (t, J = 7.2 Hz, 3H). MS (ESI): $[MH]^+$ = 408.2.

*(S)-6-(1-Hydroxybutan-2-ylamino)-3-benzyl-8-(1,3-dimethyl-1H-pyrazol-5-yl)-3H-purin-2(7H)-one (S-**11**).* White solid; 48% yield; mp 174−174 °C. ^{1}H NMR (200 MHz, DMSO-d_6) δ ppm 12.61 (bs, 1H), 7.28−7.19 (m, 6H), 6.53 (s, 1H), 5.11 (s, 2H), 4.83 (m, 1H), 4.20−4.10 (m, 1H), 3.79 (s, 3H), 3.47 (m, 2H), 2.28 (s, 3H), 1.81−1.42 (m, 2H), 0.90 (t, J = 7.2 Hz, 3H). MS (ESI): $[MH]^+$ = 408.2.

*(R,S)-6-(1-Hydroxypropan-2-ylamino)-3-allyl-8-(3-methoxy-1-methyl-1H-pyrazol-5-yl)-3H-purin-2(7H)-one (**12**).* White solid; 58% yield; mp 225 °C dec. ^{1}H NMR (200 MHz, DMSO-d_6) δ ppm 12.72 (bs, 1H), 7.53 (bs, 1H), 6.12−5.83 (m, 2H), 5.19−5.02 (m, 3H), 4.62.4.55 (m, 2H), 4.21 (m, 1H), 4.07 (s, 3H), 3.78 (s, 3H), 3.56−3.44 (m, 2H), 1.35−1.19 (m, 3H). MS (ESI): $[MH]^+$ = 360.4

*(R,S)-6-(1-Hydroxybutan-2-ylamino)-3-allyl-8-(3-methoxy-1-methyl-1H-pyrazol-5-yl)-3H-purin-2(7H)-one (**13**).* White solid; 52% yield; mp 231 °C dec. ^{1}H NMR (200 MHz, DMSO-d_6) δ ppm 12.89 (bs, 1H), 7.51 (bs, 1H), 6.11−5.82 (m, 2H), 5.19−5.02 (m, 2H), 4.99−4.80 (m, 1H), 4.59 (m, 2H), 4.07 (m, 4H), 3.77 (s, 3H), 3.62−3.41 (m, 2H),1.79−1.52 (m, 2H), 0.98−0.82 (m, 3H). MS (ESI): $[MH]^+$ = 374.4.

*(R)-6-(1-Hydroxybutan-2-ylamino)-3-allyl-8-(3-methoxy-1-methyl-1H-pyrazol-5-yl)-3H-purin-2(7H)-one (R-**13**).* White solid; 55% yield; mp 230 °C dec. ^{1}H NMR (200 MHz, $CDCl_3$) δ ppm 12.12 (bs, 1H), 7.53 (bs, 1H), 6.14 (s, 1H), 6.07−5.95 (m, 1H), 5.26−5.14 (m, 2H), 4.81−4.79 (m, 2H), 4.15 (s, 3H), 3.87 (s, 3H), 3.87−3.75 (m, 1H), 3.44 (m, 2H), 1.40−1.20 (m, 2H), 0.69−0.65 (m, 3H). MS (ESI): $[MH]^+$ = 374.4.

*(S)-6-(1-Hydroxybutan-2-ylamino)-3-allyl-8-(3-methoxy-1-methyl-1H-pyrazol-5-yl)-3H-purin-2(7H)-one (S-**13**).* White solid; 43% yield; mp 230 °C dec. ^{1}H NMR (200 MHz, $CDCl_3$) δ ppm 12.13 (bs, 1H), 7.55 (bs, 1H), 6.13 (s, 1H), 6.07−5.85 (m, 1H), 5.26−5.14 (m, 2H), 4.81−4.79 (m, 2H), 4.15 (m, 3H), 3.87 (s, 3H), 3.87−3.75 (m, 1H), 3.41 (m, 2H), 1.40−1.20 (m, 2H), 0.69−0.65 (m, 3H). MS (ESI): $[MH]^+$ = 374.4

*(R,S)-6-(1-Hydroxypropan-2-ylamino)-3-benzyl-8-(3-methoxy-1-methyl-1H-pyrazol-5-yl)-3H-purin-2(7H)-one (**14**).* White solid; 53% yield; mp 258−260 °C dec. ^{1}H NMR (400 MHz, DMSO-d_6) δ ppm 13.88 (bs, 1H), 7.51 (bs, 1H), 7.39−7.25 (m, 5H), 6.02 (s, 1H), 5.16 (s, 2H), 5.08 (s, 1H), 4.24 (m, 1H), 4.07 (s, 3H), 3.78 (s, 3H), 3.49 (m, 2H), 1.26−1.17 (m, 3H). MS (ESI): $[MH]^+$ = 410.3.

*(R)-6-(1-Hydroxypropan-2-ylamino)-3-benzyl-8-(3-methoxy-1-methyl-1H-pyrazol-5-yl)-3H-purin-2(7H)-one (R-**14**).* White solid; 57% yield; mp 257−259 °C. ^{1}H NMR (400 MHz, DMSO-d_6) δ ppm 12.83 (bs, 1H), 7.56 (bs, 1H), 7.39−7.25 (m, 5H), 6.02 (s, 1H), 5.16 (s, 2H), 5.06 (bs, 1H), 4.23 (m, 1H), 4.07 (s, 3H), 3.77 (s, 3H), 3.50 (m, 2H), 1.26−1.19 (m, 3H). MS (ESI): $[MH]^+$ = 410.3.

*(S)-6-(1-Hydroxypropan-2-ylamino)-3-benzyl-8-(3-methoxy-1-methyl-1H-pyrazol-5-yl)-3H-purin-2(7H)-one (S-**14**).* White solid; 71% yield; mp 259 °C. ^{1}H NMR (400 MHz, DMSO-d_6) δ ppm 12.93 (bs, 1H), 7.56 (bs, 1H), 7.39−7.25 (m, 5H), 6.02 (s, 1H), 5.16 (s, 2H), 5.09 (bs, 1H), 4.23 (m, 1H), 4.07 (s, 3H), 3.78 (s, 3H), 3.50 (m, 2H), 1.26−1.19 (m, 3H). MS (ESI): $[MH]^+$ = 410.3.

*(R,S)-6-(1-Hydroxybutan-2-ylamino)-3-benzyl-8-(3-methoxy-1-methyl-1H-pyrazol-5-yl)-3H-purin-2(7H)-one (**15**).* White solid; 60% yield; mp 259−260 °C. ^{1}H NMR (400 MHz, DMSO-d_6) δ ppm 12.85 (bs, 1H), 7.67 (bs, 1H), 7.40−7.30 (m, 5H), 6.02 (s, 1H), 5.17 (s, 2H), 5.02 (bs, 1H), 4.07 (m, 4H), 3.77 (s, 3H), 3.61 (m, 2H), 1.79−1.45 (m, 2H), 0.93 (m, 3H). MS (ESI): $[MH]^+$ = 424.3.

*(R,S)-6-(1-Hydroxypropan-2-ylamino)-3-allyl-8-(3-(benzyloxy)-1-methyl-1H-pyrazol-5-yl)-3H-purin-2(7H)-one (**16**).* White solid; 56% yield; mp 180−182 °C. ^{1}H NMR (200 MHz, DMSO-d_6) δ ppm 12.89 (bs, 1H), 7.43−7.35 (m, 6H), 6.02−5.87 (m, 2H), 5.16−5.10 (m, 5H),

4.58 (d, J = 4.4 Hz, 2H), 4.22 (m, 1H), 4.08 (s, 3H), 3.56−3.43 (m, 2H), 1.23 (m, 3H). MS (ESI): $[MH]^+$ = 436.5.

*(R,S)-6-(1-Hydroxybutan-2-ylamino)-3-allyl-8-(3-(benzyloxy)-1-methyl-1H-pyrazol-5-yl)-3H-purin-2(7H)-one (**17**).* White solid; 54% yield; mp 224−225 °C. ^{1}H NMR (200 MHz, DMSO-d_6) δ ppm 12.91 (bs, 1H), 7.43−7.36 (m, 6H), 6.19−5.76 (m, 2H), 5.16−5.00 (m, 4H), 4.92 (bs, 1H), 4.59 (m, 2H), 4.08 (m, 4H), 3.51−3.42 (m, 2H), 1.79−1.46 (m, 2H), 1.08−0.86 (m, 3H). MS (ESI): $[MH]^+$ = 450.5.

*(R,S)-6-(1-Hydroxypropan-2-ylamino)-3-benzyl-8-(3-(benzyloxy)-1-methyl-1H-pyrazol-5-yl)-3H-purin-2(7H)-one (**18**).* White solid; 63% yield; mp 121 °C. ^{1}H NMR (400 MHz, DMSO-d_6) δ ppm 12.83 (bs, 1H), 7.61 (bs, 1H), 7.45−7.25 (m, 10H), 6.10 (s, 1H), 5.16 (s, 4H), 5.01 (bs, 1H), 4.22 (m, 1H), 4.08 (s, 3H), 3.50 (m, 2H), 1.26−1.19 (m, 3H). MS (ESI): $[MH]^+$ = 486.3.

*(R,S)-6-(1-Hydroxybutan-2-ylamino)-3-benzyl-8-(3-(benzyloxy)-1-methyl-1H-pyrazol-5-yl)-3H-purin-2(7H)-one (**19**).* White solid; 61% yield; mp 248 °C. ^{1}H NMR (400 MHz, DMSO-d_6) δ ppm 12.98 (bs, 1H), 7.56 (bs, 1H), 7.44−7.30 (m, 10H), 6.08 (s, 1H), 5.17 (s, 2H), 5.14 (s, 2H), 5.02 (m, 1H), 4.86 (m, 1H), 4.08 (s, 3H), 3.61−3.45 (m, 2H), 1.79−1.47 (m, 2H), 0.95−9.91 (m, 3H). MS (ESI): $[MH]^+$ = 500.4.

*(R,S)-6-(1-Hydroxypropan-2-ylamino)-3-allyl-8-(1,5-dimethyl-1H-pyrazol-3-yl)-3H-purin-2(7H)-one (**20**).* Pale-yellow solid; 57% yield; mp 177−180 °C. ^{1}H NMR (200 MHz, DMSO-d_6) δ ppm 12.53 (bs, 1H), 7.26 (d, J = 7.4 Hz, 1H), 6.55 (s, 1H), 5.93−5.85 (m, 1H), 5.09−4.97 (m, 3H), 4.54 (d, J = 4.8 Hz, 2H), 4.19 (m, 1H), 3.82 (s, 3H), 3.47 (m, 2H), 2.31 (s, 3H), 1.18 (d, J = 6.8 Hz, 3H). MS (ESI): $[MH]^+$ = 344.4.

*(R,S)-6-(1-Hydroxybutan-2-ylamino)-3-allyl-8-(1,5-dimethyl-1H-pyrazol-3-yl)-3H-purin-2(7H)-one (**21**).* White solid; 52% yield; mp 169−170 °C. ^{1}H NMR (200 MHz, DMSO-d_6) δ ppm 12.61 (bs, 1H), 7.25 (d, J = 8 Hz, 1H), 6.56 (s, 1H), 6.02−5.81 (m, 1H), 5.10−4.98 (m, 3H), 4.54 (d, J = 4.8 Hz, 2H), 4.17−3.99 (m, 1H), 3.82 (s, 3H), 3.50-3.48 (m, 2H), 2.31 (s, 3H), 2.79−2.61 (m, 2H), 0.92 (t, J = 7.4 Hz, 3H). MS (ESI): $[MH]^+$ = 358.4.

*(R)-6-(1-Hydroxybutan-2-ylamino)-3-allyl-8-(1,5-dimethyl-1H-pyrazol-3-yl)-3H-purin-2(7H)-one (R-**21**).* White solid; 62% yield; mp 168−170 °C. ^{1}H NMR (400 MHz, DMSO-d_6) δ ppm 12.66 (bs, 1H), 7.21 (bs, 1H), 6.55 (s, 1H), 5.95−5.88 (m, 1H), 5.08−5.05 (m, 2H), 4.89 (bs, 1H), 4.54 (d, J = 4.8 Hz, 2H), 4.05−4.04 (m, 1H), 3.82 (s, 3H), 3.51 (m, 2H), 2.31 (s, 3H), 1.72−1.66 (m, 1H), 1.54−1.47 (m, 1H), 0.92 (t, 7.6 Hz, 3H). MS (ESI): $[MH]^+$ = 358.6.

*(S)-6-(1-Hydroxybutan-2-ylamino)-3-allyl-8-(1,5-dimethyl-1H-pyrazol-3-yl)-3H-purin-2(7H)-one (S-**21**).* White solid; 59% yield; mp 167−169 °C. ^{1}H NMR (200 MHz, DMSO-d_6) δ ppm 12.63 (bs, 1H), 7.21−7.18 (bd, J = 7.4, Hz 1H), 6.54 (s, 1H), 5.98−5.84 (m, 1H), 5.14−4.82 (m, 3H), 4.54 (d, 2H), 4.15−3.93 (m, 1H), 3.80 (s, 3H), 3.49 (m, 2H), 2.92 (s, 3H), 1.79−1.43 (m, 2H), 0.9 (t, J = 7 Hz, 3H). MS (ESI): $[MH]^+$ = 358.6.

*(R,S)-6-(1-Hydroxypropan-2-ylamino)-3-benzyl-8-(1,5-dimethyl-1H-pyrazol-3-yl)-3H-purin-2(7H)-one (**22**).* White solid; 56% yield; mp 212 °C. ^{1}H NMR (200 MHz, DMSO-d_6) δ ppm 12.84 (bs, 1H), 7.30−7.22 (m, 6H), 6.55 (s, 1H), 5.13 (s, 2H), 5.00 (bs, 1H), 4.20 (m, 1H), 3.81 (s, 3H), 3.45 (m, 2H), 2.30 (s, 3H), 1.18 (d, 3H, J = 6.6). MS (ESI): $[MH]^+$ = 394.7.

*(R,S)-6-(1-Hydroxybutan-2-ylamino)-3-benzyl-8-(1,5-dimethyl-1H-pyrazol-3-yl)-3H-purin-2(7H)-one (**23**).* White solid; 47% yield; mp 199−201 °C dec. ^{1}H NMR (200 MHz, DMSO-d_6) δ ppm 12.78 (bs, 1H), 7.31−7.24 (m, 6H), 6.56 (s, 1H), 5.14 (s, 2H), 4.90 (bs, 1H), 4.10 (m, 1H), 3.82 (s, 3H), 3.45 (m, 2H), 2.30 (s, 3H), 1.8−1.6 (m, 2H), 0.92 (t, 3H, J = 7.6). MS (ESI): $[MH]^+$ = 408.7.

*(R,S)-6-(1-Hydroxypropan-2-ylamino)-3-allyl-8-(3-methoxyisoxazol-5-yl)-3H-purin-2(7H)-one (**24**).* White solid; 64% yield; mp 289−290 °C. ^{1}H NMR (200 MHz, DMSO-d_6) δ ppm 8.52 (bs, 1H), 7.78 (bs, 1H), 6.44 (s, 1H), 6.03−5.84 (m, 1H), 5.15−5.10 (m, 3H), 4.58 (d, J = 4.8 Hz, 2H), 4.22 (m, 1H), 3.92 (s, 3H), 3.50 (m, 2H), 1.24−1.19 (m, 3H). MS (ESI): $[MH]^+$ = 347.2.

*(R,S)-6-(1-Hydroxybutan-2-ylamino)-3-allyl-8-(3-methoxyisoxazol-5-yl)-3H-purin-2(7H)-one (**25**).* White solid; 54% yield; mp 270−271 °C. ^{1}H NMR (200 MHz, DMSO-d_6) δ ppm 8.58 (bs, 1H), 7.71 (bs, 1H), 6.42 (s, 1H), 6.02−5.88 (m, 1H), 5.16−4.91 (m, 3H), 4.58 (d, J = 4.6 Hz, 2H), 4.11 (m, 1H), 3.93 (s, 3H), 3.61−3.52 (m, 2H), 1.62−1.59 (m, 2H), 0.97−0.86 (m, 3H). MS (ESI): $[MH]^+$ = 361.5.

*(R,S)-6-(1-Hydroxypropan-2-ylamino)-3-benzyl-8-(3-methoxyisoxazol-5-yl)-3H-purin-2(7H)-one (**26**).* White solid; 40% yield; mp 292−293 °C. ^{1}H NMR (200 MHz, DMSO-d_6) δ ppm 8.68 (bs, 1H), 7.78 (bs, 1H), 7.31 (m, 5H), 6.43 (s, 1H), 5.17 (s, 2H), 5.16−5.00 (m, 1H), 4.22 (m, 1H), 3.92 (s, 3H), (m, 2H), 1.35−1.24 (m, 3H). MS (ESI): $[MH]^+$ = 397.5.

*(R,S)-6-(1-Hydroxybutan-2-ylamino)-3-benzyl-8-(3-methoxyisoxazol-5-yl)-3H-purin-2(7H)-one (**27**).* White solid; 67% yield; mp 284−286 dec °C. ^{1}H NMR (200 MHz, DMSO-d_6) δ ppm 12.91 (bs, 1H), 7.80 (bs, 1H), 7.31 (m, 5H), 6.44 (s, 1H), 5.15 (s, 2H), 4.90−5.00 (s, 1H), 4.22 (m, 1H), 3.20 (s, 3H), 3.60−3.50 (m, 2H), 1.75−1.55 (m, 2H), 0.91 (t, J = 7.6 Hz, 3H). MS (ESI): $[MH]^+$ = 411.5.

General Procedure for the Preparation of 4-Allyl/benzyl-7,8-dihydro-8-methyl/ethyl-2-[(substituted)isoxazol/pyrazol-3/5-yl]-1*H*-imidazo[2,1-*i*]purin-5(4*H*)-one derivatives (28−47) . The opportune 6-(1-hydroxybutan/propan-2-ylamino)-3-allyl/benzyl-8-[(substituted)isoxazol/pyrazol-3/5-yl]-3*H*-purin-2(7*H*)-one derivative **8**−**27** (0.2 mmol) was dissolved in freshly distilled CH_2Cl_2 (7 mL) and, after cooling at 0 °C, 0.3 mL of $SOCl_2$ were added to the mixture. The reaction was stirred for further 10 min at room temperature, then heated at reflux for 18 h. The solvent and the excess of $SOCl_2$ were removed under vacuum, and the residue was purified by column chromatography on silica gel eluting with EtOAc/CH_3OH 9:1.

*(R,S)-4-Allyl-7,8-dihydro-8-methyl-2-(1,3-dimethyl-1H-pyrazol-5-yl)-1H-imidazo[2,1-i]purin-5(4H)-one (**28**).* White solid; 64% yield; mp 232 °C. ^{1}H NMR (200 MHz, DMSO-d_6) δ ppm 10.17 (bs, 1H), 6.40 (s, 1H), 6.05−5.83 (m, 1H), 5.22−5.13 (m, 2H), 4.62 (d, J = 5 Hz, 2H), 4.32 (m, 2H), 4.15 (s, 3H), 3.78 (m, 1H), 2.14 (s, 3H), 1.34 (d, J = 5.6 Hz, 3H). MS (ESI): $[MH]^+$ = 326.3. Anal. ($C_{16}H_{19}N_7O$) C, H, N.

*(R)-4-Allyl-7,8-dihydro-8-methyl-2-(1,3-dimethyl-1H-pyrazol-5-yl)-1H-imidazo[2,1-i]purin-5(4H)-one (R-**28**).* White solid; 64% yield; mp 233 °C. ^{1}H NMR (200 MHz, DMSO-d_6) δ ppm 10.17 (bs, 1H), 6.40 (s, 1H), 5.97−5.88 (m, 1H), 5.23−5.13 (m, 2H), 4.62 (d, J = 5.2 Hz, 2H), 4.37−4.22 (m, 2H), 4.15 (s, 3H), 3.75−3.67 (m, 1H), 2.14 (s, 3H), 1.34 (d, J = 5.8 Hz, 3H). MS (ESI): $[MH]^+$ = 325.8. Anal. ($C_{16}H_{19}N_7O$) C, H, N.

*(S)-4-Allyl-7,8-dihydro-8-methyl-2-(1,3-dimethyl-1H-pyrazol-5-yl)-1H-imidazo[2,1-i]purin-5(4H)-one (S-**28**).* White solid; 48% yield; mp 233 °C. ^{1}H NMR (200 MHz, DMSO-d_6) δ ppm 10.17 (bs, 1H), 6.40 (s, 1H), 6.02−5.88 (m, 1H), 5.22−5.13 (m, 2H), 4.62 (d, J = 5.2 Hz, 2H), 4.39−4.22 (m, 1H), 4.15 (s, 3H), 3.75−3.67 (m, 1H), 2.14 (s, 3H), 1.34 (d, J = 5.8 Hz, 3H). MS (ESI): $[MH]^+$ = 325.8. Anal. ($C_{16}H_{19}N_7O$) C, H, N.

*(R,S)-4-Allyl-8-ethyl-7,8-dihydro-2-(1,3-dimethyl-1H-pyrazol-5-yl)-1H-imidazo[2,1-i]purin-5(4H)-one (**29**).* White solid; 51% yield; mp 188 °C. ^{1}H NMR (200 MHz, DMSO-d_6) δ ppm 10.17 (bs, 1H), 6.40 (s, 1H), 6.02−5.88 (m, 1H), 5.22−5.13 (m, 2H), 4.62 (d, J = 5.2 Hz, 2H), 4.25−4.22 (m, 2H), 4.15 (s, 3H), 3.75−3.67 (m, 1H), 2.14 (s, 3H), 1.68 (m, 2H), 0.94 (t, J = 7.4 Hz, 3H). MS (ESI): $[MH]^+$ = 340.8. Anal. ($C_{17}H_{21}N_7O$) C, H, N.

*(R,S)-4-Benzyl-7,8-dihydro-8-methyl-2-(1,3-dimethyl-1H-pyrazol-5-yl)-1H-imidazo[2,1-i]purin-5(4H)-one (**30**).* White solid; 57% yield; mp 244 °C. ^{1}H NMR (400 MHz, DMSO-d_6) δ ppm 1.07 (bs, 1H), 7.38−7.24 (m, 5H), 6.41 (s, 1H), 5.19 (s, 2H), 4.38−4.17 (m, 2H), 3.73 (s, 3H), 3.69−3.60 (m, 1H), 2.26 (s, 3H), 1.32 (d, J = 6.4 Hz, 3H). MS (ESI): $[MH]^+$ = 376.6. Anal. ($C_{20}H_{21}N_7O$) C, H, N

*(R,S)-4-Benzyl-8-ethyl-7,8-dihydro-2-(1,3-dimethyl-1H-pyrazol-5-yl)-1H-imidazo[2,1-i]purin-5(4H)-one (**31**).* White solid; 48% yield; mp 295 °C. ^{1}H NMR (200 MHz, DMSO-d_6) δ ppm 10.12 (bs, 1H), 7.42−7.28 (m, 5H), 6.68 (s, 1H), 5.19 (s, 2H), 4.20−4.00 (m, 5H), 3.80 (m, 1H), 2.15 (s, 3H), 1.65 (m, 2H), 0.95 (t, J = 7.2 Hz, 3H). MS (ESI): $[MH]^+$ = 390.2. Anal. ($C_{21}H_{23}N_7O$) C, H, N.

*(R)-4-Benzyl-8-ethyl-7,8-dihydro-2-(1,3-dimethyl-1H-pyrazol-5-yl)-1H-imidazo[2,1-i]purin-5(4H)-one (R-**31**).* White solid; 48% yield; mp 294 °C. ^{1}H NMR (200 MHz, DMSO-d_6) δ ppm 10.12 (bs, 1H), 7.39−7.27 (m, 5H), 6.42 (s, 1H), 5.20 (s, 2H), 4.20−4.18 (m, 2H), 3.73 (m, 4H), 2.26 (s, 3H), 1.65 (m, 2H), 0.94 (t, J = 7.2 Hz, 3H). MS (ESI): $[MH]^+$ = 390.2. Anal. ($C_{21}H_{23}N_7O$) C, H, N.

*(S)-4-Benzyl-8-ethyl-7,8-dihydro-2-(1,3-dimethyl-1H-pyrazol-5-yl)-1H-imidazo[2,1-i]purin-5(4H)-one (S-**31**).* White solid; 43% yield; mp 295 °C. ^{1}H NMR (200 MHz, DMSO-d_6) δ ppm 10.21 (bs, 1H), 7.35−7.27 (m, 5H), 6.42 (s, 1H), 5.20 (s, 2H), 4.17 (m, 2H), 3.73 (m, 4H), 2.26 (s, 3H), 1.79−1.62 (m, 2H), 0.94 (t, J = 7.2 Hz, 3H). MS (ESI): $[MH]^+$ = 390.2. Anal. ($C_{21}H_{23}N_7O$) C, H, N.

*(R,S)-4-Allyl-7,8-dihydro-2-(3-methoxy-1-methyl-1H-pyrazol-5-yl)-8-methyl-1H-imidazo[2,1-i]purin-5(4H)-one (**32**).* White solid; 55% yield; mp 121 °C. ^{1}H NMR (400 MHz, DMSO-d_6) δ ppm 10.17 (bs, 1H), 5.99 (s, 1H), 5.95−5.91 (m, 1H), 5.20−5.14 (m, 2H), 4.62 (d, J = 5.2 Hz, 2H), 4.4.38−4.25 (m, 2H), 4.10 (s, 3H), 3.77 (s, 3H), 3.75−3.70 (m, 1H), 1.34 (d, J = 6 Hz, 3H). MS (ESI): $[MH]^+$ = 342.4. Anal. ($C_{16}H_{19}N_7O_2$) C, H, N.

*(R,S)-4-Allyl-8-ethyl-7,8-dihydro-2-(3-methoxy-1-methyl-1H-pyrazol-5-yl)-1H-imidazo[2,1-i]purin-5(4H)-one (**33**).* White solid; 47% yield; mp 133 °C. ^{1}H NMR (400 MHz, DMSO-d_6) δ ppm 10.23 (bs, 1H), 6.00 (s, 1H), 5.98−5.89 (m, 1H), 5.20−5.14 (m, 2H), 4.62 (d, J = 5.2 Hz, 2H), 4.26−4.24 (m, 2H), 4.10 (s, 3H), 3.83−3.78 (m, 1H), 3.77 (s, 3H), 1.68 (m, 2H), 0.95 (t, J = 7.2 Hz, 3H). MS (ESI): $[MH]^+$ = 356.2. Anal. ($C_{17}H_{21}N_7O_2$) C, H, N.

*(R)-4-Allyl-8-ethyl-7,8-dihydro-2-(3-methoxy-1-methyl-1H-pyrazol-5-yl)-1H-imidazo[2,1-i]purin-5(4H)-one (R-**33**).* White solid; 54% yield; mp 133 °C. ^{1}H NMR (200 MHz, DMSO-d_6) δ ppm 10.23 (bs, 1H), 6.00 (s, 1H), 5.98−5.89 (m, 1H), 5.22−5.13 (m, 2H), 4.62 (d, J = 5.2 Hz, 2H), 4.26−4.24 (m, 2H), 4.10 (s, 3H), 3.83−3.78 (m, 1H), 3.77 (s, 3H), 1.68 (m, 2H), 0.95 (t, J = 7.2 Hz, 3H). MS (ESI): $[MH]^+$ = 356.2. Anal. ($C_{17}H_{21}N_7O_2$) C, H, N.

*(S)-4-Allyl-8-ethyl-7,8-dihydro-2-(3-methoxy-1-methyl-1H-pyrazol-5-yl)-1H-imidazo[2,1-i]purin-5(4H)-one (S-**33**).* White solid; 51% yield; mp 133 °C. ^{1}H NMR (200 MHz, DMSO-d_6) δ ppm 10.23 (bs, 1H), 6.02 (s, 1H), 5.98−5.89 (m, 1H), 5.18−5.13 (m, 2H), 4.62 (d, J = 5.2 Hz, 2H), 4.26−4.24 (m, 2H), 4.10 (s, 3H), 3.83−3.78 (m, 1H), 3.77 (s, 3H), 1.68 (m, 2H), 0.95 (t, J = 7.2 Hz, 3H). MS (ESI): $[MH]^+$ = 356.2. Anal. ($C_{17}H_{21}N_7O_2$) C, H, N.

*(R,S)-4-Benzyl-7,8-dihydro-2-(3-methoxy-1-methyl-1H-pyrazol-5-yl)-8-methyl-1H-imidazo[2,1-i]purin-5(4H)-one (**34**).* White solid; 57% yield; mp 243 °C. ^{1}H NMR (400 MHz, DMSO-d_6) δ ppm 10.21 (bs, 1H), 7.44−7.25 (m, 5H), 5.98 (s, 1H), 5.19 (s, 2H), 4.35−4.22 (m, 2H), 4.10 (s, 3H), 3.76 (s, 3H), 3.70−3.66 (m, 1H), 1.32 (d, J = 6.4 Hz, 3H). MS (ESI): $[MH]^+$ = 392.2. Anal. ($C_{20}H_{21}N_7O_2$) C, H, N.

*(R)-4-Benzyl-7,8-dihydro-2-(3-methoxy-1-methyl-1H-pyrazol-5-yl)-8-methyl-1H-imidazo[2,1-i]purin-5(4H)-one (R-**34**).* White solid; 67% yield; mp 242 °C. ^{1}H NMR (400 MHz, DMSO-d_6) δ ppm 10.19 (bs, 1H), 7.42−7.23 (m, 5H), 5.98 (s, 1H), 5.18 (s, 2H), 4.35−4.24 (m, 2H), 4.08 (s, 3H), 3.75 (s, 3H), 3.73−3.68 (m, 1H), 1.32 (d, J = 6 Hz, 3H). MS (ESI): $[MH]^+$ = 392.2. Anal. ($C_{20}H_{21}N_7O_2$) C, H, N.

*(S)-4-Benzyl-7,8-dihydro-2-(3-methoxy-1-methyl-1H-pyrazol-5-yl)-8-methyl-1H-imidazo[2,1-i]purin-5(4H)-one (S-**34**).* White solid; 60% yield; mp 244 °C. ^{1}H NMR (400 MHz, DMSO-d_6) δ ppm 10.23 (bs, 1H), 7.43−7.24 (m, 5H), 6.06 (s, 1H), 5.20 (s, 2H), 4.39−4.26 (m, 2H), 4.08 (s, 3H), 3.76 (s, 3H), 3.73−3.71 (m, 1H), 1.34 (d, J = 6.4 Hz, 3H). MS (ESI): $[MH]^+$ = 392.2. Anal. ($C_{20}H_{21}N_7O_2$) C, H, N.

*(R,S)-4-Benzyl-8-ethyl-7,8-dihydro-2-(3-methoxy-1-methyl-1H-pyrazol-5-yl)-1H-imidazo[2,1-i]purin-5(4H)-one (**35**).* White solid; 53% yield; mp 140 °C. ^{1}H NMR (400 MHz, DMSO-d_6) δ ppm 10.38 (bs, 1H), 7.43−7.25 (m, 5H), 6.08 (s, 1H), 5.21 (s, 2H), 4.27−4.23 (m, 2H), 4.08 (s, 3H), 3.81−3.80 (m, 1H), 3.76 (s, 3H), 1.70−1.66 (m, 2H), 0.93 (t, J = 7.2 Hz, 3H). MS (ESI): $[MH]^+$ = 406.2. Anal. ($C_{21}H_{23}N_7O_2$) C, H, N.

*(R,S)-4-Allyl-2-(3-(benzyloxy)-1-methyl-1H-pyrazol-5-yl)-7,8-dihydro-8-methyl-1H-imidazo[2,1-i]purin-5(4H)-one (**36**).* White solid; 59% yield; mp 214 °C. ^{1}H NMR (400 MHz, DMSO-d_6) δ ppm 10.18 (bs, 1H), 7.45−7.38 (m, 5H), 6.03 (s, 1H), 5.98−5.84 (m, 1H), 5.20−5.14 (m, 4H), 4.62 (d, J = 5.2 Hz, 2H), 4.37−4.25 (m, 2H), 4.11 (s, 3H), 3.74−3.70 (m, 1H), 1.34 (d, J = 6.4 Hz, 3H). MS (ESI): $[MH]^+$ = 418.2. Anal. ($C_{22}H_{23}N_7O_2$) C, H, N.

*(R,S)-4-Allyl-2-(3-(benzyloxy)-1-methyl-1H-pyrazol-5-yl)-8-ethyl-7,8-dihydro-1H-imidazo[2,1-i]purin-5(4H)-one (**37**).* White solid; 60% yield; mp 223 °C. ^{1}H NMR (400 MHz, DMSO-d_6) δ ppm 10.25 (bs, 1H), 7.43−7.38 (m, 5H), 6.03 (s, 1H), 5.98−5.91 (m, 1H), 5−20−5.14 (m, 4H), 4.62 (d, J = 5.6 Hz, 2H), 4.28−4.21 (m, 2H), 4.11 (s, 3H), 3.81−3.78 (m, 1H), 1.70−1.66 (m, 2H), 0.94 (t, J = 7.2 HZ, 3H). MS (ESI): $[MH]^+$ = 432.2. Anal. ($C_{23}H_{25}N_7O_2$) C, H, N.

*(R,S)-4-Benzyl-2-(3-(benzyloxy)-1-methyl-1H-pyrazol-5-yl)-7,8-dihydro-8-methyl-1H-imidazo[2,1-i]purin-5(4H)-one (**38**).* White solid; 42% yield; mp 143 °C. ^{1}H NMR (400 MHz, DMSO-d_6) δ ppm 10.22 (bs, 1H), 7.45−7.31 (m, 10H), 6.05 (s, 1H), 5.20 (s, 2H), 5.14 (s, 2H), 4.37−4.26 (m, 2H), 4.11 (s, 3H), 3.75−3.71 (m, 1H), 1.34 (d, J = 6 Hz, 3H). MS (ESI): $[MH]^+$ = 468.2. Anal. ($C_{26}H_{25}N_7O_2$) C, H, N.

*(R,S)-4-Benzyl-2-(3-(benzyloxy)-1-methyl-1H-pyrazol-5-yl)-8-ethyl-7,8-dihydro-1H-imidazo[2,1-i]purin-5(4H)-one (**39**).* White solid; 49% yield; mp 120 °C. ^{1}H NMR (400 MHz, DMSO-d_6) δ ppm 10.22 (bs, 1H), 7.45−7.29 (m, 10H), 6.05 (s, 1H), 5.20 (s, 2H), 5.14 (s, 2H), 4.26−4.20 (m, 2H), 3.82−3.78 (m, 2H), 4.11 (s, 1H), 3.82−3.78 (m,1H), 1.70−1.66 (m, 2H), 0.94 (t, J = 7.2 Hz, 3H). MS (ESI): $[MH]^+$ = 482.2. Anal. ($C_{27}H_{27}N_7O_2$) C, H, N.

*(R,S)-4-Allyl-7,8-dihydro-8-methyl-2-(1,5-dimethyl-1H-pyrazol-3-yl)-1H-imidazo[2,1-i]purin-5(4H)-one (**40**).* White solid; 49% yield; mp 214 °C dec. ^{1}H NMR (400 MHz, DMSO-d_6) δ ppm 10.43 (bs, 1H), 6.41 (s, 1H), 5.98−5.91 (m, 1H), 5.14−5.11 (m, 2H), 4.60 (d, J = 5.2 Hz, 2H), 4.39−4.18 (m, 2H), 3.74 (s, 3H), 3.67−3.62 (m, 1H), 2.26 (s, 3H), 1.31 (d, J = 6 Hz, 3H). MS (ESI): $[MH]^+$ = 326.2. Anal. ($C_{16}H_{19}N_7O$) C, H, N.

*(R,S)-4-Allyl-8-ethyl-7,8-dihydro-2-(1,5-dimethyl-1H-pyrazol-3-yl)-1H-imidazo[2,1-i]purin-5(4H)-one (**41**).* White solid; 46% yield; mp 249 °C. ^{1}H NMR (400 MHz, DMSO-d_6) δ ppm 10.43 (bs, 1H), 6.45 (s, 1H), 5.98−5.91 (m, 1H), 5.15−5.11 (m, 2H), 4.61 (d, J = 5.2 Hz, 2H), 4.22−4.20 (m, 2H), 3.76 (m, 4H), 2.27 (s, 3H), 1.68−1.65 (m, 2H), 0.95 (t, J = 7.2 Hz, 3H). MS (ESI): $[MH]^+$ = 340.2. Anal. ($C_{17}H_{21}N_7O$) C, H, N.

*(R)-4-Allyl-8-ethyl-7,8-dihydro-2-(1,5-dimethyl-1H-pyrazol-3-yl)-1H-imidazo[2,1-i]purin-5(4H)-one (R-**41**).* White solid; 48% yield; mp 249 °C. ^{1}H NMR (400 MHz, DMSO-d_6) δ ppm 10.11 (bs, 1H), 6.41 (s, 1H), 5.99−5.87 (m, 1H), 5.14−5.09 (m, 2H), 4.60 (d, J = 4.8 Hz, 2H), 4.17−4.60 (m, 2H), 3.80−3.70 (m, 4H), 2.26 (s, 3H), 1.65 (m, 2H), 0.94 (t, J = 7.2 Hz, 3H). MS (ESI): $[MH]^+$ = 339.9. Anal. ($C_{17}H_{21}N_7O$) C, H, N.

*(S)-4-Allyl-8-ethyl-7,8-dihydro-2-(1,5-dimethyl-1H-pyrazol-3-yl)-1H-imidazo[2,1-i]purin-5(4H)-one (S-**41**).* White solid; 47% yield; mp 249 °C. ^{1}H NMR (200 MHz, DMSO-d_6) δ ppm 10.08 (bs, 1H), 6.41 (s, 1H), 6.00−5.88 (m, 1H), 5.16−5.07 (m, 2H), 4.60 (d, J = 4.8 Hz, 2H), 4.20−4.17 (m, 2H), 3.74 (s, 3H), 3.70 (m, 1H), 2.26 (s, 3H), 1.68−1.62 (m, 2H), 0.94 (t, J = 7.2 Hz, 3H). MS (ESI): $[MH]^+$ = 340.2. Anal. ($C_{17}H_{21}N_7O$) C, H, N.

*(R,S)-4-Benzyl-7,8-dihydro-8-methyl-2-(1,5-dimethyl-1H-pyrazol-3-yl)-1H-imidazo[2,1-i]purin-5(4H)-one (**42**).* White solid; 65% yield; mp

245 °C. ^{1}H NMR (200 MHz, DMSO-d_6) δ ppm 10.20 (bs, 1H), 7.35−7.27 (m, 5H), 6.42 (s, 1H), 5.20 (s, 2H), 4.40−4.20 (m, 2H), 3.80−3.60 (m, 4H), 2.26 (s, 3H), 1.31 (d, J = 5.8 Hz, 3H). MS (ESI): $[MH]^+$ = 376.9. Anal. ($C_{20}H_{21}N_7O$) C, H, N.

*(R,S)-4-Benzyl-8-ethyl-7,8-dihydro-2-(1,5-dimethyl-1H-pyrazol-3-yl)-1H-imidazo[2,1-i]purin-5(4H)-one (**43**).* White solid; 61% yield; mp 275 °C. ^{1}H NMR (200 MHz, DMSO-d_6) δ ppm 10.20 (bs, 1H), 7.35−7.27 (m, 5H), 6.42 (s, 1H), 5.20 (s, 2H), 4.20−4.10 (m, 2H), 3.80−3.60 (m, 4H), 2.26 (s, 3H), 1.70−1.60 (m, 2H), 0.94 (t, J = 7.2 Hz, 3H). MS (ESI): $[MH]^+$ = 390.9. Anal. ($C_{21}H_{23}N_7O$) C, H, N.

*(R,S)-4-Allyl-7,8-dihydro-2-(3-methoxyisoxazol-5-yl)-8-methyl-1H-imidazo[2,1-i]purin-5(4H)-one (**44**).* White solid; 57% yield; mp 169 °C. ^{1}H NMR (200 MHz, DMSO-d_6) δ ppm 10.74 (bs, 1H), 6.53 (s, 1H), 5.93−5.88 (m, 1H), 5.21−5.13 (m, 2H), 4.63 (d, J = 4.8 Hz, 2H), 4.45−4.26 (m, 2H), 3.94 (s, 3H), 3.80−3.72 (m, 1H), 1.36 (d, J = 6 Hz, 3H). MS (ESI): $[MH]^+$ = 329.2. Anal. ($C_{15}H_{16}N_6O_3$) C, H, N.

*(R,S)-4-Allyl-8-ethyl-7,8-dihydro-2-(3-methoxyisoxazol-5-yl)-1H-imidazo[2,1-i]purin-5(4H)-one (**45**).* White solid; 51% yield; mp 171 °C dec. ^{1}H NMR (200 MHz, DMSO-d_6) δ ppm 10.79 (bs, 1H), 6.50 (s, 1H), 6.02−5.88 (m, 1H), 5.20−5.12 (m, 2H), 4.63 (d, J = 4.8 Hz, 2H), 4.30−4.27 (m, 2H), 3.94 (s, 3H), 3.84−3.82 (m, 1H), 1.74−1.67 (m, 2H), 0.95 (t, J = 7.2 Hz, 3H). MS (ESI): $[MH]^+$ = 343.3. Anal. ($C_{16}H_{18}N_6O_3$) C, H, N.

*(R,S)-4-Benzyl-8-methyl-7,8-dihydro-2-(3-methoxyisoxazol-5-yl)-1H-imidazo[2,1-i]purin-5(4H)-one (**46**).* White solid; 38% yield; mp 111 °C. ^{1}H NMR (200 MHz, DMSO-d_6) δ ppm 10.64 (bs, 1H), 7.41−7.21 (m, 5H), 6.47 (s, 1H), 5.22 (s, 2H), 4.43−4.26 (m, 2H), 3.94 (m, 4H), 1.36 (d, J = 5.6 Hz, 3H). MS (ESI): $[MH]^+$ = 379.1. Anal. ($C_{19}H_{18}N_6O_3$) C, H, N.

*(R,S)-4-Benzyl-7,8-dihydro-8-ethyl-2-(3-methoxyisoxazol-5-yl)-1H-imidazo[2,1-i]purin-5(4H)-one (**47**).* White solid; 39% yield; mp 157 °C. ^{1}H NMR (200 MHz, $CDCl_3$) δ ppm 10.64 (bs, 1H), 7.60−7.56 (m, 2H), 7.32−7.28 (m, 3H), 6.46 (s, 1H), 5.35 (s, 2H), 4.63−4.31 (m, 2H), 4.01 (s, 3H), 3.90−3.85 (m, 1H), 1.60−1.40 (m, 2H), 0.74 (t, J = 7.6 Hz, 3H). MS (ESI): $[MH]^+$ = 393.1. Anal. ($C_{20}H_{20}N_6O_3$) C, H, N.

Evaluation of Affinity (K_i) and Potency (IC_{50}) of the Novel Adenosine Compounds. *CHO Membranes Preparation.* The human A_1, A_{2A}, A_{2B}, and A_3 receptors have been transfected in CHO cells according with the method previously described.[49] The cells were grown adherently and maintained in Dulbecco's Modified Eagles Medium with nutrient mixture F12 (DMEM/F12) without nucleosides, containing 10% fetal calf serum, penicillin (100 U/mL), streptomycin (100 μg/mL), L-glutamine (2 mM), and Geneticin (G418, 0.2 mg/mL) at 37 °C in 5% CO_2, 95% air. Cells were split 2 or 3 times weekly at a ratio between 1:5 and 1:20. For membrane preparation, the culture medium was removed and the cells were washed with PBS and scraped off T75 flasks in ice-cold hypotonic buffer (5 mM Tris HCl, 2 mM EDTA, pH 7.4). The cell suspension was homogenized with Polytron, and the homogenate was spun for 10 min at 1000g. The supernatant was then centrifuged for 30 min at 100000g. The membrane pellet was suspended in: (a) 50 mM Tris HCl buffer pH 7.4 for A_1 adenosine receptors, (b) 50 mM Tris HCl, 10 mM $MgCl_2$ buffer pH 7.4 for A_{2A} adenosine receptors, and (c) 50 mM Tris HCl, 10 mM $MgCl_2$, 1 mM EDTA buffer pH 7.4 for A_3 adenosine receptors. The cell suspension were incubated with 2 UI/mL of adenosine deaminase for 30 min at 37 °C. The membrane preparation was used to perform binding experiments.

Human Cloned A_1, A_{2A}, and A_3 Adenosine Receptor Binding Assay. All synthesized compounds have been tested for their affinity at human A_1, A_{2A}, and A_3 adenosine receptors. Displacement binding experiments of [^{3}H]-DPCPX (1nM) to hA_1CHO membranes (50 μg of protein/assay) and at least 6−8 different concentrations of antagonists studied were performed for 120 min at 25 °C. Nonspecific binding was determined in the presence of 1 μM of DPCPX, and this was always $\leq$10% of the total binding.[50] Inhibition binding experiments of [^{3}H]-ZM 241385 (2nM) to hA_{2A}CHO membranes (50 μg of protein/assay) and at least 6−8 different concentrations of antagonists studied were performed for 60 min at 4 °C. Nonspecific binding was determined in the presence of 1 μM ZM 241385 and was about 20% of total binding.[51] Competition binding experiments of [^{3}H]-MRE 3008F20 (1nM) to hA_3CHO membranes (50 μg of protein/assay) and at least 6−8 different concentrations of examined ligands were performed for 120 min at 4 °C. Nonspecific binding was defined as binding in the presence of 1 μM MRE 3008F20 and was about 25% of total binding.[52] Bound and free radioactivity were separated by filtering the assay mixture through Whatman GF/B glass fiber which were washed three times with ice-cold buffer. Filter bound radioactivity was measured by scintillation spectrometry (Tri Carb Packard 2500-TR) after addition of Aquassure liquid.

Measurement of Cyclic AMP Levels in CHO Cells Transfected with Human A2B and A3 Adenosine Receptors. CHO cells transfected with human A_{2B} or A_3 adenosine receptors were washed with phosphate-buffered saline and diluted trypsine and centrifuged for 10 min at 200g. The pellet containing CHO cells (1 × 106 cells/assay) was suspended in 0.5 mL of incubation mixture (mM): NaCl 15, KCl 0.27, NaH_2PO_4 0.037, $MgSO_4$ 0.1, $CaCl_2$ 0.1, Hepes 0.01, $MgCl_2$ 1, glucose 0.5, pH 7.4 at 37 °C, 2 IU/mL adenosine deaminase, and 4-(3-butoxy-4-methoxybenzyl)-2-imidazolidinone (Ro 20-1724) as phosphodiesterase inhibitor and preincubated for 10 min in a shaking bath at 37 °C. The potencies of antagonists to hA_{2B} adenosine receptors were determined by antagonism of NECA (100 nM)-induced stimulation of cyclic AMP levels.[53] The potencies of antagonists to hA3 adenosine receptors were determined in the presence of Forskolin 1 μM by antagonism of Cl-IB-MECA (100 nM)-induced inhibition of cyclic AMP levels.[52] The reaction was terminated by the addition of cold 6% trichloroacetic acid (TCA). The TCA suspension was centrifuged at 2000g for 10 min at 4 °C, and the supernatant was extracted four times with water saturated diethyl ether. The final aqueous solution was tested for cyclic AMP levels by a competition protein binding assay. Samples of cyclic AMP standard (0−10 pmoles) were added to each test tube containing the incubation buffer (trizma base 0.1 M, aminophylline 8.0 mM, 2 mercaptoethanol 6.0 mM, pH 7.4) and [^{3}H] cyclic AMP in a total volume of 0.5 mL. The binding protein, previously prepared from beef adrenals, was added to the samples previously incubated at 4 °C for 150 min and after the addition of charcoal were centrifuged at 2000g for 10 min. The clear supernatant was counted in a 2500-TR Packard scintillation counter.

Data Analysis. The protein concentration was determined according to a Bio-Rad method[54] with bovine albumin as a standard reference. Inhibitory binding constants, K_i values, were calculated from those of IC_{50} according to Cheng and Prusoff equation[55] $K_i = IC_{50}/(1 + [C^*]/K_D^*)$, where $[C^*]$ is the concentration of the radioligand and K_D^* its dissociation constant. A weighted nonlinear least-squares curve fitting program LIGAND[56] was also used for computer analysis of inhibition experiments. Potency values (IC_{50}) obtained in cyclic AMP assays were calculated by nonlinear regression analysis using the equation for a sigmoid concentration−response curve (Graph PAD Prism, San Diego, CA, USA). Affinity values are expressed as geometric mean, with 95% or 99% confidence limits in parentheses and IC_{50} values are expressed as the arithmetic mean ± SEM.

Molecular Modeling. The homology model of the hA_1 and hA_3 ARs were built using Schrödinger Prime[57] software accessible through the Maestro interface.[58] Unless otherwise stated, default parameters were used throughout. The sequence of the hA1 (P30542) and hA_3 (P33765) ARs were aligned against the sequence of hA_{2A} AR (P29274). Alignment of anchor residues within each TM domain were attained according to the sequence alignment suggested by Moro and co-workers (Figure 6).[45]

During the homology model building, Prime keeps the backbone rigid for the cases in which the backbone does not need to be

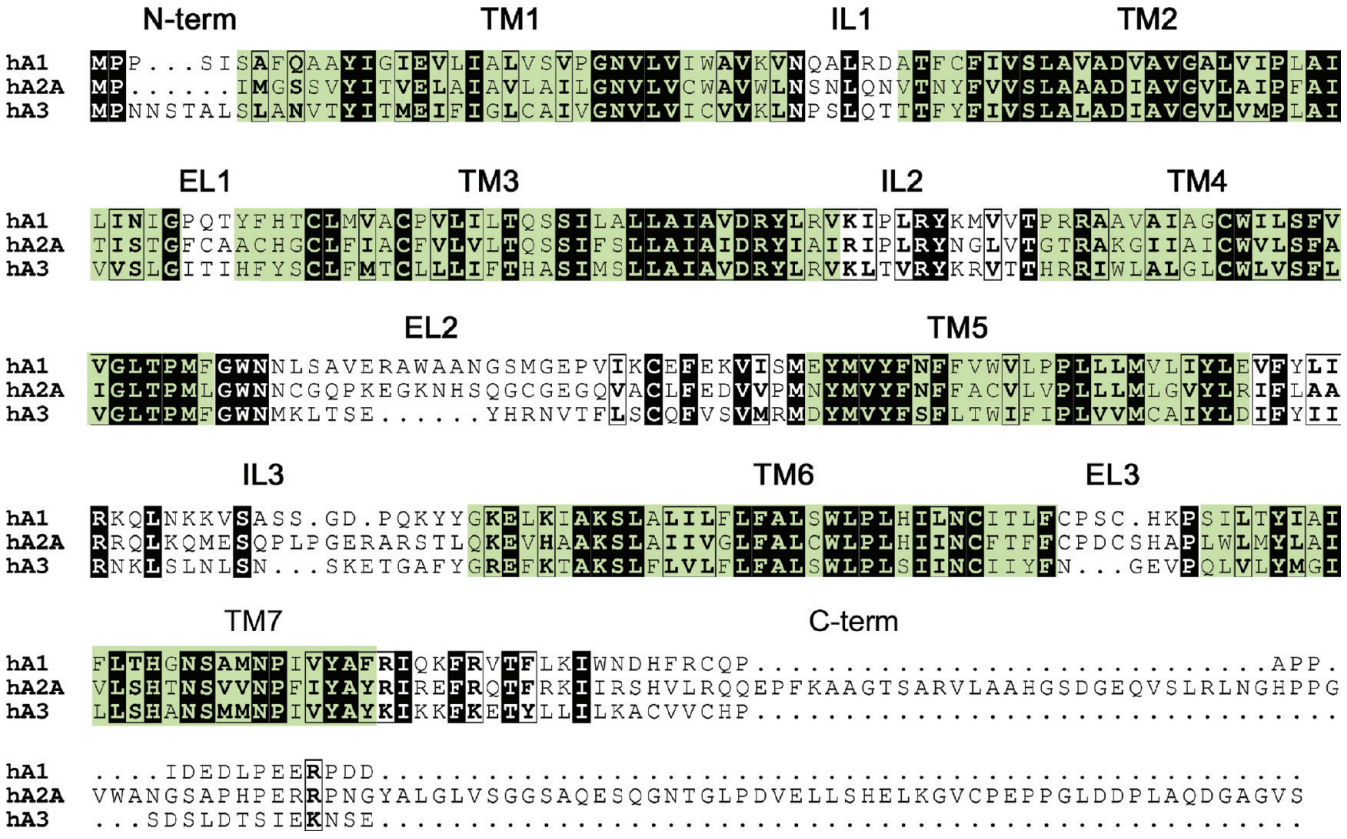

Figure 6. Sequence alignment of hA_1, hA_3 and hA_{2A} ARs. Conserved and semiconserved residues are identified by black boxes and bold characters, respectively. Transmembrane portions are identified by green boxes.

reconstructed due to gaps in the alignment. The loop refinements were carried out using Prime with default parameter settings, if not mentioned otherwise. Prior to refinement, the protein structures were subjected to a protein preparation step to reorientate side chain hydroxyl groups and alleviate potential steric clashes. The implemented loop modeling protocol consists of several steps.[59] First, large numbers of loops are created by a conformational search in dihedral angle space. Clustering of loop conformations and side chain optimization is being used to select representative solutions. On the basis of the user parameters, a limited number of structures is then processed using complete energy minimization. The top ranked solution in terms of Prime energy was considered best. The short loops (ELI and ELIII) were refined using default sampling rates in the initial step, while the extended, highest sampling rate was chosen for the larger amino acid loops (ELII). Side chains were unfrozen within 7.5 Å of the corresponding loop, and the energy cutoff was set to 10 kcal.

The Glide program of the Schrodinger package was used to dock *R*-**33** to the hA_1, hA_{2A}, and hA_3 ARs structures and compounds **29**, *S*-**33**, **35**, *R*-**41**, and **45** to the hA_3AR. The receptor grid generation were performed for the box with a center in the putative binding site. The size of the box was determined automatically. The extra precision mode (XP) of Glide was used for the docking. The ligand scaling factor was set to 1.0. The geometry of the ligand binding site of the complex between *R*-**33** and the three receptors was then optimized. The binding site was defined as *R*-**33** and all amino acid residues located within 8 Å from the ligand All the receptor residues located within 2 Å from the binding site were used as a shell. The following parameters of energy minimization were used: OPLS2005 force field, water was used as an implicit solvent, a maximum of 5000 iterations of the Polak−Ribier conjugate gradient minimization method was used with a convergence threshold of 0.01 kJ 3 mol^{-1} $Å^{-1}$. All complexes pictures were rendered employing the UCSF Chimera software.[60]

■ ASSOCIATED CONTENT

Ⓢ Supporting Information. Additional molecular modeling pictures for **35**, *S*-**33**, **29**, *R*-**41**, and **45**. This material is available free of charge via the Internet at http://pubs.acs.org.

■ AUTHOR INFORMATION

Corresponding Author

*For P.G.B.: phone, +39-0532-455921; Fax, +39-0532-455921; E-mail, baraldi@dns.unife.it. For D.P.: phone, +39-0532-455302; fax, +39-0532-455921; E-mail, prtdle@unife.it.

■ ACKNOWLEDGMENT

We thank King Pharmaceuticals, Inc., Research & Development, 4000 CentreGreen Way, Suite 300, Cary, North Carolina 27513, for financial support. We also thank Prof. Karl-Norbert Klotz for cDNA encoding the human adenosine receptors.

■ ABBREVIATIONS USED

ARs, adenosine receptors; cAMP, 3′-5′-cyclic adenosine monophosphate; DMF, dimethylformamide; CHO, Chinese hamster ovary; Cl-IB-MECA, 2-chloro-N^6-(3-iodobenzyl)adenosine-5′-*N*-methylcarboxamide; DMEM, Dulbecco's Modified Eagles Medium; DMSO, dimethylsulfoxide; EDAC, 1-ethyl-3-[3 (dimethylamino)-

propyl]carbodiimide hydrochloride; EDTA, ethylenediaminetetraacetic acid; HOBt, hydroxybenzotriazole; NECA, 5′-(*N*-ethylcarboxamido)adenosine; PBS, phosphate buffered saline; PDB, Protein Data Bank; TCA, trichloroacetic acid

REFERENCES

(1) Fredholm, B. B.; Ijzerman, A. P.; Jacobson, K. A.; Klotz, K.-N.; Linden, J. Nomenclature and classification of adenosine receptors. *Pharm. Rev.* **2001**, *53*, 527–552.

(2) Jacobson, K. A. Adenosine A_3 receptors: novel ligands and paradoxical effects. *Trends Pharmacol. Sci.* **1998**, *19*, 184–191.

(3) Merighi, S.; Mirandola, P.; Varani, K.; Gessi, S.; Leung, E.; Baraldi, P. G.; Tabrizi, M. A.; Borea, P. A. A glance at adenosine receptors: novel target for antitumor therapy. *Pharmacol. Ther.* **2003**, *100*, 31–48.

(4) Fishman, P.; Bar-Yehuda, S.; Barer, F.; Ohana, G. A_3 adenosine receptors: new targets for cancer therapy and chemoprotection. *Drug Dev. Res.* **2000**, *50*, 101–117.

(5) Ohana, G.; Bar-yehuda, S.; Barer, F.; Fishman, P. Differential effect of adenosine on tumor and normal cell growth: focus on the A_3 adenosine receptor. *J. Cell. Phys.* **2001**, *186*, 19–23.

(6) Gessi, S.; Varani, K.; Merighi, S.; Morelli, A.; Ferrari, D.; Leung, E.; Baraldi, P. G.; Spalluto, G.; Borea, P. A. Pharmacological and biochemical characterization of A_3 adenosine receptors in Jurkat T cells. *Br. J. Pharmacol.* **2001**, *134*, 116–126.

(7) Merighi, S.; Varani, K.; Gessi, S.; Cattabriga, E.; Iannotta, V.; Uloglou, C.; Leung, E.; Borea, P. A. Pharmacological and biochemical characterization of adenosine receptors in the human malignant melanoma A375 cell line. *Br. J. Pharmacol.* **2001**, *134*, 1215–1226.

(8) Gessi, S.; Cattabriga, E.; Avitabile, A.; Gafa', R.; Lanza, G.; Cavazzini, L.; Bianchi, N.; Gambari, R.; Feo, C.; Liboni, A.; Gullini, S.; Leung, E.; Mac-Lennan, S.; Borea, P. A. Elevated expression of A_3 adenosine receptors in human colorectal cancer is reflected in peripheral blood cells. *Clin. Canc. Res.* **2004**, *10*, 5895–5901.

(9) Schlotzer-Schrehardt, U.; Zenkel, M.; Decking, U.; Haubs, D.; Kruse, F. E.; Junemann, A.; Coca-Prados, M.; Naumann, G. O. Selective upregulation of the A_3 adenosine receptor in eyes with pseudoexfoliation syndrome and glaucoma. *Invest. Ophthalmol. Vis. Sci.* **2005**, *46*, 2023–2034.

(10) Okamura, T.; Kurogi, Y.; Hashimoto, K.; Sato, S.; Nishikawa, H.; Kiryu, K.; Nagao, Y. Structure−activity relationships of adenosine A_3 receptor ligands: new potential therapy for the treatment of glaucoma. *Bioorg. Med. Chem. Lett.* **2004**, *14*, 3775–3779.

(11) Avila, M. Y.; Stone, R. A.; Civan, M. M. Knockout of A_3 adenosine receptors reduces mouse intraocular pressure. *Invest. Ophthalmol. Vis. Sci.* **2002**, *43*, 3021–3026.

(12) Müller, C. E. Medicinal chemistry of adenosine A_3 receptor ligands. *Curr. Top. Med. Chem.* **2003**, *3*, 445–462.

(13) Jacobson, K. A.; Klutz, A. M.; Tosh, D. K.; Ivanov, A. A.; Preti, D.; Baraldi, P. G. Medicinal chemistry of the A_3 adenosine receptor: agonists, antagonists, and receptor engineering. *Handb. Exp. Pharmacol.* **2009**, *193*, 123–59.

(14) Jung, K.-Y.; Kim, S.-K.; Gao, Z.-G.; Gross, A. S.; Melman, N.; Jacobson, K. A.; Kim, Y. C. Structure−activity relationships of thiazole and thiadiazole derivatives as potent and selective human adenosine A_3 receptor antagonists. *Bioorg. Med. Chem.* **2004**, *12*, 613–623.

(15) Van Rhee, A. M.; Jiang, J. L.; Melman, N.; Olah, M. E.; Stiles, G. L.; Jacobson, K. A. Interaction of 1,4-dihydropyridine and pyridine derivatives with adenosine receptors: selectivity for A_3 receptors. *J. Med. Chem.* **1996**, *39*, 2980–2989.

(16) Li, A. H.; Moro, S.; Forsyth, N.; Melman, N.; Ji, X. D.; Jacobson, K. A. Synthesis, CoMFA analysis, and receptor docking of 3,5-diacyl-2,4-dialkylpyridine derivatives as selective A_3 adenosine receptor antagonists. *J. Med. Chem.* **1999**, *42*, 706–721.

(17) Cosimelli, B.; Greco, G.; Ehlardo, M.; Novellino, E.; Da Settimo, F.; Taliani, S.; La Motta, C.; Bellandi, M.; Tuccinardi, T.; Martinelli, A.; Ciampi, O.; Trincavelli, M. L.; Martini, C. Derivatives of 4-amino-6-hydroxy-2-mercaptopyrimidine as novel, potent, and selective A_3 adenosine receptor antagonists. *J. Med. Chem.* **2008**, *51*, 1764–1770.

(18) Karton, Y.; Jiang, J. L.; Ji, X.-D.; Melman, N.; Olah, M. E.; Stiles, G. L.; Jacobson, K. A. Synthesis and biological activities of flavonoid derivatives as A_3 adenosine receptor antagonists. *J. Med. Chem.* **1996**, *39*, 2293–2301.

(19) Van Muijlwijk-Koezen, J. E.; Timmerman, H.; Link, R.; von der Goot, H.; Menge, W. M. P. B.; Frijtag von Drabbe Künzel, J.; de Groote, M.; Ijzerman, A. P. Isoquinoline and quinazoline urea analogues as antagonists for the human adenosine A_3 receptor. *J. Med. Chem.* **2000**, *43*, 2227–2238.

(20) Perreiram, M.; Jiang, J.; Klutz, A. M.; Gao, Z. G.; Shainberg, A.; Lu, C.; Thomas, C. J.; Jacobson, K. A. Reversine and its 2-substituted adenine derivatives as potent and selective A_3 adenosine receptor antagonists. *J. Med. Chem.* **2005**, *48*, 4910–4918.

(21) Colotta, V.; Catarzi, D.; Varano, F.; Capelli, F.; Lenzi, O.; Filacchioni, G.; Martini, C.; Trincavelli, L.; Ciampi, O.; Pugliese, A. M.; Pedata, F.; Schiesaro, A.; Morizzo, E.; Moro, S. New 2-arylpyrazolo[3,4-*c*]-quinoline derivatives as potent and selective human A_3 adenosine receptor antagonists. Synthesis, pharmacological evaluation, and ligand−receptor modeling studies. *J. Med. Chem.* **2007**, *50*, 4061–4074.

(22) Baraldi, P. G.; Tabrizi, M. A.; Preti, D.; Bovero, A.; Fruttarolo, F.; Romagnoli, R.; Zaid, N. A.; Moorman, A. R.; Varani, K.; Borea, P. A. New 2-arylpyrazolo[4,3-*c*]quinoline derivatives as potent and selective human A_3 adenosine receptor antagonists. *J. Med. Chem.* **2005**, *48*, 5001–5008.

(23) Colotta, V.; Catarzi, D.; Varano, F.; Lenzi, O.; Filacchioni, G.; Martini, C.; Trincavelli, L.; Ciampi, O.; Traini, C.; Pugliese, A. M.; Pedata, F.; Morizzo, E.; Moro, S. Synthesis, ligand−receptor modeling studies and pharmacological evaluation of novel 4-modified-2-aryl-1,2,4-triazolo[4,3-*a*]quinoxalin-1-one derivatives as potent and selective human A_3 adenosine receptor antagonists. *Bioorg. Med. Chem.* **2008**, *16*, 6086–6102.

(24) Baraldi, P. G.; Cacciari, B.; Borea, P. A.; Varani, K.; Pastorin, G.; Da Ros, T.; Spalluto, G. Pyrazolo-triazolo-pyrimidine derivatives as adenosine receptor antagonists: a possible template for adenosine receptor subtypes? *Curr. Pharm. Des.* **2002**, *8*, 99–110.

(25) Okamura, T.; Kurogi, Y.; Hashimoto, K.; Sato, S.; Nishikawa, H.; Kiryu, K.; Nagao, Y. Structure−activity relationships of adenosine A_3 receptor ligands: new potential therapy for the treatment of glaucoma. *Bioorg. Med. Chem. Lett.* **2004**, *14*, 3775–3779.

(26) Priego, E. M.; von Frijtag Drabbe Kuenzel, J.; Ijzerman, A. P.; Camarasa, M. J.; Pérez-Pérez, M. J. Pyrido[2,1-*f*]purine-2,4-dione derivatives as a novel class of highly potent human A_3 adenosine receptor antagonists. *J. Med. Chem.* **2002**, *45*, 3337–3344.

(27) Baraldi, P. G.; Preti, D.; Tabrizi, M. A.; Fruttarolo, F.; Romagnoli, R.; Zaid, N. A.; Moorman, A. R.; Merighi, S.; Varani, K.; Borea, P. A. New pyrrolo[2,1-*f*]purine-2,4-dione and imidazo[2,1-*f*]-purine-2,4-dione derivatives as potent and selective human A_3 adenosine receptor antagonists. *J. Med. Chem.* **2005**, *48*, 4697–4701.

(28) Baraldi, P. G.; Preti, D.; Tabrizi, M. A.; Romagnoli, R.; Saponaro, G.; Baraldi, S.; Botta, M.; Bernardini, C.; Tafi, A.; Tuccinardi, T.; Martinelli, A.; Varani, K.; Borea, P. A. Structure−activity relationship studies of a new series of imidazo[2,1-*f*]purinones as potent and selective A_3 adenosine receptor antagonists. *Bioorg. Med. Chem.* **2008**, *16*, 10281–10294.

(29) Gao, Z. G.; Kim, S. K.; Biadatti, T.; Chen, W.; Lee, K.; Barak, D.; Kim, S. G.; Johnson, C. R.; Jacobson, K. A. Structural determinants of A_3 adenosine receptor activation: nucleoside ligands at the agonist/antagonist boundary. *J. Med. Chem.* **2002**, *45*, 4471–4484.

(30) Gao, Z. G.; Joshi, B. V.; Klutz, A. M.; Kim, S. K.; Lee, H. W.; Kim, H. O.; Jeong, L. S.; Jacobson, K. A. Conversion of A_3 adenosine receptor agonists into selective antagonists by modification of the 5′-ribofuranuronamide moiety. *Bioorg. Med. Chem. Lett.* **2006**, *16*, 596–601.

(31) Jeong, L. S.; Choe, S. A.; Gunaga, P.; Kim, H. O.; Lee, H. W.; Lee, S. K.; Tosh, D. K.; Patel, A.; Palaniappan, K. K.; Gao, Z. G.;

Jacobson, K. A.; Moon, H. R. Discovery of a new nucleoside template for human A_3 adenosine receptor ligands: D-4′-thioadenosine derivatives without 4′-hydroxymethyl group as highly potent and selective antagonists. *J. Med. Chem.* **2007**, *50*, 3159–3162.

(32) Suzuki, F.; Shimada, J.; Nonaka, H.; Ishii, A.; Shiozaki, S.; Ichikawa, S.; Ono, E. 7,8-Dihydro-8-ethyl-2-(3-noradamantyl)-4-propyl-1*H*-imidazo[2,1-*i*]purin-5(4*H*)-one: a potent and water-soluble adenosine A_1 antagonist. *J. Med. Chem.* **1992**, *35*, 3578–3581.

(33) Vu, C. B.; Kiesman, W. F.; Conlon, P. R.; Lin, K-C; Tam, M.; Petter, R. C.; Smits, G.; Lutterodt, F.; Jin, X.; Chen, L.; Zhang, J. Tricyclic imidazoline derivatives as potent and selective adenosine A_1 receptor antagonists. *J. Med. Chem.* **2006**, *49*, 7132–7139.

(34) Saki, M.; Tsumuki, H.; Nonaka, H.; Shimada, J.; Ichimura, M. KF26777 (2-(4-bromophenyl)-7,8-dihydro-4-propyl-1*H*-imidazo[2,1-*i*]purin-5(4*H*)-one dihydrochloride), a new potent and selective adenosine A_3 receptor antagonist. *Eur. J. Pharmacol.* **2002**, *444*, 133–144.

(35) Müller, C. E.; Thorand, M.; Qurishi, R.; Diekmann, M.; Jacobson, K. A.; Padgett, W. L.; Daly, J. W. Imidazo[2,1-*i*]purin-5-ones and related tricyclic water-soluble purine derivatives: potent A_{2A}- and A_3-adenosine receptor antagonists. *J. Med. Chem.* **2002**, *45*, 3440–3450.

(36) Müller, C. E.; Diekmann, M.; Thorand, M.; Ozola, V. [^{3}H]8-Ethyl-4-methyl-2-phenyl-(8*R*)-4,5,7,8-tetrahydro-1*H*-imidazo[2,1-*i*]-purin-5-one ([^{3}H]PSB-11), a novel high affinity antagonist radioligand for human A_3 adenosine receptors. *Bioorg. Med. Chem. Lett.* **2002**, *12*, 501–503.

(37) Ozola, V.; Thorand, M.; Diekmann, M.; Qurishi, R.; Schumacher, B.; Jacobson, K. A.; Muller, C. E. 2-Phenylimidazo[2,1-*i*]purin-5-ones: structure−activity relationships and characterization of potent and selective inverse agonists at human A_3 adenosine receptors. *Bioorg. Med. Chem.* **2003**, *11*, 347–356.

(38) Baraldi, P. G.; Tabrizi, M. A.; Preti, D.; Bovero, A.; Romagnoli, R.; Fruttarolo, F.; Zaid, N. A.; Moorman, A. R.; Varani, K.; Gessi, S.; Merighi, S.; Borea, P. A. Design, synthesis, and biological evaluation of new 8-heterocyclic xanthine derivatives as highly potent and selective human A_{2B} adenosine receptor antagonists. *J. Med. Chem.* **2004**, *47*, 1434–1447.

(39) Kim, Y.-C.; Ji, X.; Melman, N.; Linden, J.; Jacobson, K. A. Anilide derivatives of an 8-phenylxanthine carboxylic congener are highly potent and selective antagonists at human A_{2B} adenosine receptors. *J. Med. Chem.* **2000**, *43*, 1165–1172.

(40) Shimada, J.; Kuroda, T; Suzuki, F. A convenient synthesis of tricyclic purine derivatives. *J. Heterocycl. Chem.* **1993**, *30*, 241–246.

(41) Papesch, V.; Schroeder, E. F. Synthesis of 1-mono- and 1,3-substituted 6-amino-uracils. Diuretic activity. *J. Org. Chem.* **1951**, *16*, 1879–1890.

(42) Schmidt, A.; Habeck, T.; Kindermann, M. K.; Nieger, M. New pyrazolium-carboxylates as structural analogues of the pseudo-cross-conjugated betainic alkaloid nigellicine. *J. Org. Chem.* **2003**, *68*, 5977–5982.

(43) Frey, M.; Jäger, V. Synthesis of N-substituted muscimol derivatives including *N*-glycylmuscimol. *Synthesis* **1985**, *12*, 1100–1104.

(44) Jaakola, V. P.; Griffith, M. T.; Hanson, M. A.; Cherezov, V.; Chien, E. Y. T.; Lane, J. R.; IJzerman, A. P.; Stevens, R. C. The 2.6 angstrom crystal structure of a human A_{2A} adenosine receptor bound to an antagonist. *Science* **2008**, *322*, 1211–1217.

(45) Lenzi, O.; Colotta, V.; Catarzi, D.; Varano, F.; Poli, D.; Filacchioni, G.; Varani, K.; Vincenzi, F.; Borea, P. A.; Paoletta, S.; Morizzo, E.; Moro, S. 2-Phenylpyrazolo[4,3-*d*]pyrimidin-7-one as a new scaffold to obtain potent and selective human A_3 adenosine receptor antagonists: new insights into the receptor−antagonist recognition. *J. Med. Chem.* **2009**, *52*, 7640–7652.

(46) Tosh, D. K.; Chinn, M.; Ivanov, A. A.; Klutz, A. M.; Gao, Z.-G.; Jacobson, K. A. Functionalized congeners of A_3 adenosine receptor-selective nucleosides containing a bicyclo[3.1.0]hexane ring system. *J. Med. Chem.* **2009**, *52*, 7580–7592.

(47) Gao, Z.-G.; Chen, A.; Barak, D.; Kim, S.-K.; Muller, C. E.; Jacobson, K. A. Identification by site-directed mutagenesis of residues involved in ligand recognition and activation of the human A_3 adenosine receptor. *J. Biol. Chem.* **2002**, *277*, 19056–19063.

(48) Kim, J.; Wess, J.; van Rhee, M.; Schoneberg, T.; Jacobson, K. A. Site-directed mutagenesis identifies residues involved in ligand recognition in the human A_{2A} adenosine receptor. *J. Biol. Chem.* **1995**, *270*, 13987–13997.

(49) Klotz, K. N.; Hessling, J.; Hegler, J.; Owman, C.; Kull, B.; Fredholm, B. B.; Lohse, M. J. Comparative pharmacology of human adenosine receptor subtypes—characterization of stably transfected receptors in CHO cells. *Naunyn-Schmiedeberg's Arch. Pharm.* **1998**, *357*, 1–9.

(50) Borea, P. A.; Dalpiaz, A.; Varani, K.; Gessi, S.; Gilli, G. Binding thermodynamics of adenosine A_{2A} receptor ligands. *Biochem. Pharmacol.* **1995**, *49*, 461–469.

(51) Borea, P. A.; Dalpiaz, A.; Varani, K.; Gessi, S.; Gilli, G. Binding thermodynamics at A_1 and A_{2A} adenosine receptors. *Life Sci.* **1996**, *59*, 1373–1388.

(52) Varani, K.; Merighi, S.; Gessi, S.; Klotz, K. N.; Leung, E.; Baraldi, P. G.; Cacciari, B.; Romagnoli, R.; Spalluto, P.; Borea, P. A. [^{3}H]-MRE3008F20: a novel antagonist radioligand for the pharmacological and biochemical characterization of human A_3 adenosine receptors. *Mol. Pharmacol.* **2000**, *57*, 968–975.

(53) Varani, K.; Gessi, S.; Merighi, S.; Vincenzi, F.; Cattabriga, E.; Benini, A.; Klotz, K. N.; Baraldi, P. G.; Tabrizi, M. A.; Mac Lennan, S.; Leung, E.; Borea, P. A. Pharmacological characterization of novel adenosine ligands in recombinant and native human A_{2B} receptors. *Biochem. Pharmacol.* **2005**, *70*, 1601–1612.

(54) Bradford, M. M. A rapid and sensitive method for the quantification of microgram quantities of protein utilizing the principle of protein dye-binding. *Anal. Biochem.* **1976**, *72*, 248–254.

(55) Cheng, Y. C.; Prusoff, W. H. Relationships between the inhibition constant (K_i) and the concentration of inhibitor which causes 50% inhibition (IC_{50}) of an enzymatic reaction. *Biochem. Pharmacol.* **1973**, *22*, 3099–3108.

(56) Munson, P. J.; Rodbard, D. Ligand: a versatile computerized approach for the characterization of ligand binding systems. *Anal. Biochem.* **1980**, *107*, 220–239.

(57) *Prime, version 2.0*; Schrödinger, LLC: New York, NY, 2005.

(58) *Maestro, version 8.5*; Schrödinger, LLC: New York, NY, 2006.

(59) Jacobson, M. P.; Pincus, D. L.; Rapp, C. S.; Day, T. J.; Honig, B.; Shaw, D. E.; Friesner, R. A. A hierarchical approach to all-atom protein loop prediction. *Proteins* **2004**, *55*, 351–367.

(60) Pettersen, E. F.; Goddard, T. D.; Huang, C. C.; Couch, G. S.; Greenblatt, D. M.; Meng, E. C.; Ferrin, T. E. UCSF Chimera—a visualization system for exploratory research and analysis. *J. Comput. Chem.* **2004**, *25*, 1605–1612.